



Department of Electrical and Electronic Engineering  
Part IV Project Report 2003

---

# An Inductively Coupled Universal Battery Charger

---

Author: Robert Coup  
Project Partner: Monique Ryan  
Supervisor: Dr. Patrick Hu

---

## **Abstract**

This project's objective was to create an inductively coupled universal battery charger, supporting the simultaneous charging of multiple batteries, and the most common rechargeable battery types.

The design consists of a base station containing a parallel resonant converter and a tuned pickup circuit. Increasing the operating frequency has advantages although can make tuning and stability difficult. The charger operates at 85kHz, compared to a typical IPT system at 10-40kHz.

A bidirectional communications system operates between the base station and connected pickups, and uses the same inductive link that transfers power. Forward communication uses amplitude shift keying to modulate data, while for reverse communication the pickup varies the load to change the reflected voltage at the base station.

The base station is responsible for controlling the total system power, the charging algorithms for each connected battery, and reporting to a PC. The pickup measures battery parameters and controls the power delivered to an individual battery as instructed by the base station.

A maximum of 16W can be delivered to a passive load, sufficient for the application. The bidirectional communications operates at 300bps, with a bit error rate of <0.3%.

## **Declaration of Originality**

This report is my own unaided work and was not copied from nor written in collaboration with any other person.

Signed: \_\_\_\_\_ (*Robert Coup*)

Date: 15 September 2003

## Acknowledgments

I would like to thank the following people for their support, advice, and assistance during the work on this project.

Dr. Patrick Hu, Dept. of Electrical and Electronic Engineering, for his advice and guidance on the development of the project, and for letting me talk him into changing the direction of the project. His thesis is a brilliant introduction and reference to inductive power transfer.

Monique Ryan, for her enthusiasm and commitment. It makes life a hundred times easier when you have a project partner who is so committed. She's always smiling, and has an infinite amount of patience in explaining concepts to me, toiling away to get a circuit working, and humouring my unfeasible ideas.

Debbie Low, for her wonderful support. It is brilliant to have someone to rant to, or just take time out with, and who can always make you smile. She's also the best proof-reader of reports.

## Table of Contents

Abstract .....	i
Declaration of Originality .....	ii
Acknowledgments .....	iii
Table of Contents .....	iv
List of Figures .....	vi
List of Tables .....	vii
Glossary .....	viii
1. Introduction .....	1
1.1. The 'need' .....	1
1.2. Goals and Objectives .....	1
2. Background .....	2
2.1. Inductive Power Transfer .....	2
2.2. IPT Communications .....	2
3. System Design .....	4
3.1. Overview .....	4
3.2. Control .....	5
3.2.1. Component Selection .....	6
3.2.2. Base Station Software Implementation .....	7
3.2.3. Pickup Software Implementation .....	8
4. Inductive Power Transfer .....	10
4.1. Base Station Design .....	10
4.1.1. Power Supply .....	10
4.1.2. Resonant Converter .....	11
4.2. Battery Pickup Design .....	14
4.3. Results and Performance .....	14
4.3.1. Resonant Converter .....	14
4.3.2. Pickup .....	15
4.3.3. Power Efficiency .....	16
4.4. High Frequency Operation .....	16
5. Communications .....	18
5.1. Primary to Secondary .....	18
5.2. Secondary to Primary .....	20
5.3. Envelope Detection .....	20
5.4. Protocol Design .....	20
5.4.1. Network Topology .....	21
5.4.2. Packet Format .....	21
5.4.3. Device Discovery .....	22
5.5. Results and Performance .....	22

---

6.	Battery Charging .....	25
6.1.	Charging Control.....	25
6.1.1.	Battery Measurements .....	25
6.1.2.	Current and Voltage Control.....	26
6.2.	Battery Technologies .....	26
6.2.1.	Nickel Cadmium.....	26
6.2.2.	Nickel Metal Hydride.....	27
6.2.3.	Lithium Ion.....	27
6.2.4.	Sealed Lead Acid.....	27
6.3.	Results and Performance.....	27
7.	Future Developments .....	29
7.1.	Inductive Power Transfer.....	29
7.2.	Battery Charging .....	29
7.3.	Communications .....	29
8.	Conclusions .....	31
9.	References.....	32
10.	Bibliography .....	33
Appendix A.	Device Discovery .....	34
Appendix B.	CRC Algorithm .....	35
Appendix C.	ADC Data Capture Algorithm .....	36
Appendix D.	Data Commands and Packets .....	37
Appendix E.	Current and Voltage Control Algorithm .....	38
Appendix F.	Base Station Circuit Schematic .....	39
Appendix G.	Pickup Circuit Schematic.....	40

## List of Figures

Figure 2.1: Overview of an IPT system. ....	2
Figure 3.1: Overview of the battery charger operation.....	4
Figure 3.2: Base Station functional block diagram.....	5
Figure 3.3: Pickup functional block diagram.....	5
Figure 3.4: Simplified flowchart of the Base Station software.....	8
Figure 3.5: Simplified flowchart of the pickup software. ....	9
Figure 4.1: Schematic and operation of the Buck converter.....	11
Figure 4.2: Simplified schematic of Base Station.....	11
Figure 4.3: Graphs of the switching operation of the resonant converter. $V_1$ and $V_2$ are the voltages across MOSFETs S1 and S2 respectively. $V_{ac}$ is the voltage across the output of the resonant converter.....	12
Figure 4.4: Simplified schematic of the Zero Voltage Switching circuit. ...	13
Figure 4.5: Simplified schematic of the battery pickup design. ....	14
Figure 4.6: Oscilloscope capture of the MOSFET switching in the resonant converter.....	15
Figure 4.7: Power transfer efficiency for the system under different passive loads, with the pickup Boost converter operating at several duty cycles.....	16
Figure 5.1: Sending and receiving a Phase Shift Keying modulated signal.	18
Figure 5.2: Sending and receiving a Frequency Shift Keying modulated signal. ....	19
Figure 5.3: Sending and receiving an Amplitude Shift Keying modulated signal. ....	19
Figure 5.4: Simplified schematic showing the operation of the envelope detector. ....	19
Figure 5.5: Communications data packet format. ....	21
Figure 5.6: Modulation Indexes of the communications at different frequencies. ....	23
Figure 5.7: Modulation of a 1kHz square wave onto the power waveform from the primary side with the output of the secondary envelope detector. ....	24
Figure 5.8: Modulation of a 4.8kHz square wave onto the power waveform from the secondary side with the output of the primary envelope detector.	24
Figure 6.1: Simplified schematic of the battery voltage and charge current measurement circuits.....	25
Figure 6.2: Simplified schematic of the Boost converter circuit. ....	26

## List of Tables

Table 4.1: Control signals and operation of the Zero Voltage switching logic. .....	13
Table 4.2: Comparison of actual and expected parameter values for Resonant Converter.....	15
Table 4.3: Parameter values for the pickup circuit. ....	15
Table 5.1: Forward communications bit error rates.....	22
Table 5.2: Reverse communication bit error rates. ....	23
Table 6.1: Battery parameters measurement accuracy.....	27



## Glossary

**Boost Converter** - A transformerless switching power supply that outputs a voltage higher than its input voltage.

**Buck Converter** - A transformerless switching power supply that outputs a voltage lower than its input voltage.

**EMI** – Electromagnetic Interference. An electromagnetic disturbance that degrades the performance of electrical equipment.

**Envelope Detector** – a circuit to remove the underlying carrier signal from a modulated waveform. For amplitude modulated signals this consists of a low pass filter.

**IPT** – Inductive Power Transfer. The transfer of power over large air gaps using magnetic coupling.

**Li-Ion** – Lithium Ion. A rechargeable battery technology offering very high energy density and long life. Currently the most popular battery type for new mobile devices.

**MOSFET** – Metal Oxide Semiconductor Field Effect Transistor. These transistors are commonly used for switching in digital and analogue circuits.

**NiCd** – Nickel Cadmium. A rechargeable battery technology from the 1960s, which became the first mainstream portable rechargeable battery.

**NiMH** – Nickel Metal Hydride. A rechargeable battery technology developed in the 1980s, offering higher energy density than NiCd technology.

**Optocoupler** – A device designed to pass a data signal between two isolated sections of a circuit.

**PWM** – Pulse Width Modulation. A method of modulating data by varying the duty cycle of a constant frequency signal, commonly used in control applications.

**SLA** – Sealed Lead Acid. A rechargeable battery technology for use in low cost applications where weight and size is not critical.

**ZVS** – Zero Voltage Switching. A technique used in IPT systems to control the MOSFET switching. It detects the zero-crossings of the voltage in the resonant tank and switches the MOSFETs alternately at these crossing points.

## 1. Introduction

The aim of this project was to create a contactless universal battery charger using inductive power transfer. The battery charger should be capable of charging the most common battery types found in portable devices today. In addition, the charging should be controlled from the base station and a bidirectional communication system between the pickups and base station should be developed.

In 2002, a related project “An Automatic Contactless Battery Charger for Robot Power Supplies” developed an IPT charger for a small robot. [1, 2] This project expands on that work by moving the focus towards a more universal system and attempting to improve the design.

The project was undertaken by Robert Coup and Monique Ryan as part of the Part IV program in the Department of Electrical and Electronic Engineering at the University of Auckland. The project was supervised by Dr. Patrick Hu with Dr. Partha Roop as the second examiner.

### 1.1. The ‘need’

As the number of portable and mobile devices increases – phones, digital assistants, laptops, MP3 players, digital cameras, and GPS units – they all need to be charged, using different adaptors specific to each device. In future the system could be used to charge any of these just by sitting devices with a small built-in pickup onto the charger.

### 1.2. Goals and Objectives

The overall objective of the project was to create a universal battery charger, which can charge any popular type of battery using inductive power transfer.

The base station should control the simultaneous charging of multiple devices, while minimizing power usage. While it should operate completely autonomously, a facility for sending information to a PC should be implemented.

The pickup should measure various battery characteristics (cell voltage, charging current, and temperature) and report these to the base station. It should also control the voltage and charging current as instructed by the base station. It is important for the pickup to be as small and as low-cost as possible. In order to reduce the size, the inductive power transfer operates at a high frequency, meaning a decrease in size of the base station and pickup components.

The bidirectional data communication between the base station and pickups should be conducted via the same inductive power transfer link that provides power to the pickup circuits.

## 2. Background

### 2.1. Inductive Power Transfer

Inductive Power Transfer (IPT) refers to the concept of transferring electrical power between two isolated circuits across an air gap. While based on the work and concepts developed by pioneers such as Faraday and Ampere, it is only recently that IPT has been developed into working systems.

IPT has a number of advantages over other power transfer methods – it is unaffected by dirt, dust, water, or chemicals. In situations such as coal mining IPT prevents sparks and other hazards. As the coupling is magnetic, there is no risk of electrocution even when used in high power systems. This makes IPT very suitable for transport systems where vehicles follow a fixed track, such as in factory materials handling. [3]

Essentially, an IPT system can be divided into two parts; primary and secondary. The primary side of the system is made up of a resonant power supply and a coil. This power supply produces a high frequency sinusoidal current in the coil. The secondary side (or 'pickup') has a smaller coil, and a converter to produce a DC voltage. This is illustrated in Figure 2.1.

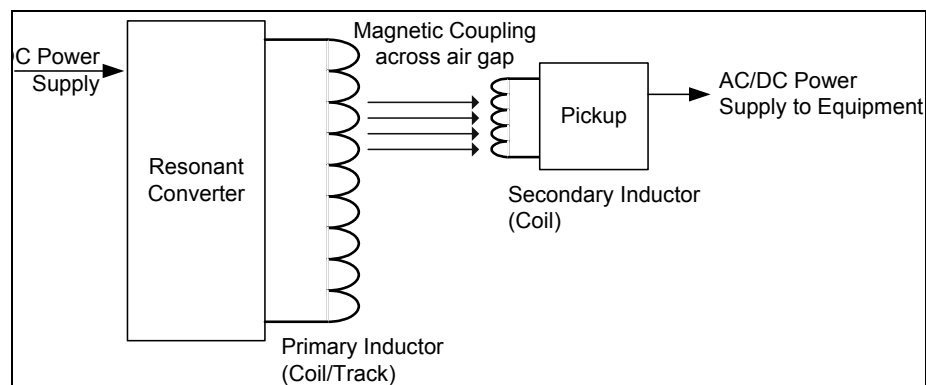


Figure 2.1: Overview of an IPT system.

IPT has the potential to impact our everyday lives. One day it may be possible to power all cars using IPT from cables running under the roads. Automatic guided vehicles used for materials handling, powered via IPT, are already in use in a number of large manufacturing operations worldwide.

### 2.2. IPT Communications

Adding communications to an IPT system allows increased functionality, as well as enhanced control and optimisation of the power transfer. Current research is beginning to focus on communication over the IPT channel in conjunction with the power transfer.

A number of applications have been developed using unidirectional IPT communications from the base station to the pickup. In some applications this is sufficient, but in others responses from the pickups are required. Typically, these reverse communications have been implemented using another IPT link or using radio or Infrared solutions.

In the biomedical area a number of similar systems exist with telemeters implanted in the body being powered by and communicating with outside devices. [4, 5] Generally these operate at much higher frequencies than IPT. The principles used in developing bidirectional communications for these telemeters can be applied to IPT systems. Developing a working bidirectional communications system across the IPT power link could be used for many existing and new IPT projects.

### 3. System Design

#### 3.1. Overview

The operation of the battery charging system is shown in Figure 3.1. The base station coordinates and controls all the charging operations for any connected pickups with batteries. When a battery is placed on the base station it automatically picks up the energy and turns itself on. The base station detects it within a few seconds using a device discovery protocol, and begins charging.

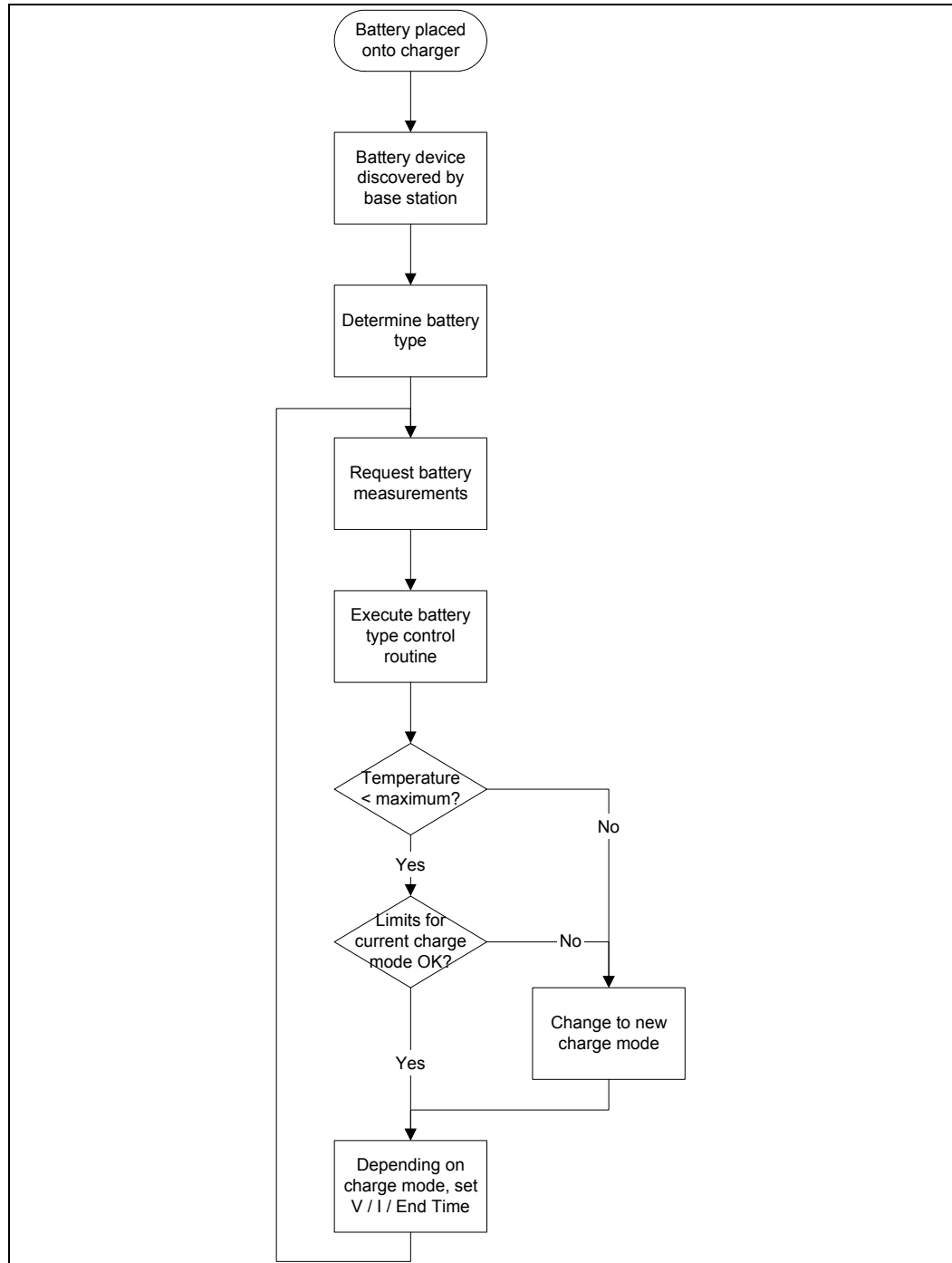


Figure 3.1: Overview of the battery charger operation.

The base station is connected to the power supply and controls the IPT system. It coordinates communication, controls the battery charging, and updates the PC with status information. The pickup is connected to a battery and regulates the power transferred across the IPT channel, measures battery parameters, communicates with the base station and controls the flow of current to the battery. The main functional blocks of the base station and pickup components are shown in Figure 3.2 and Figure 3.3 respectively.

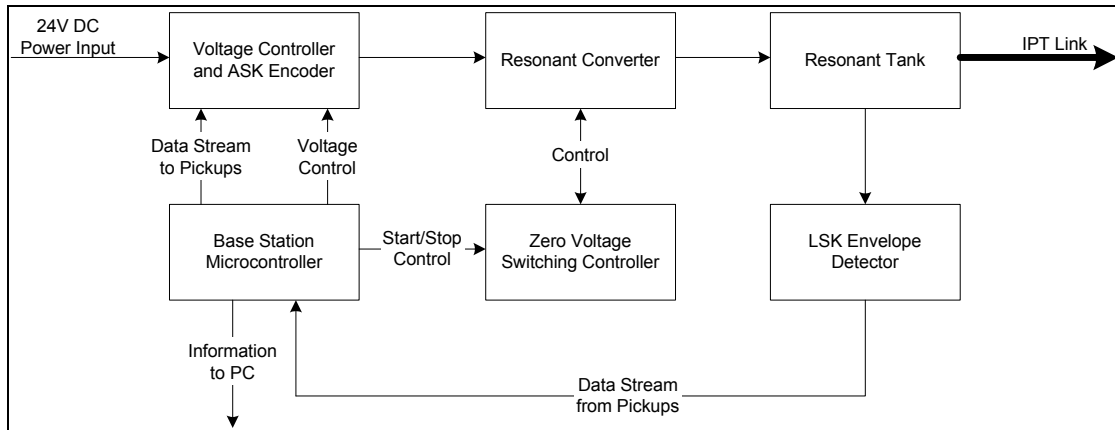


Figure 3.2: Base Station functional block diagram.

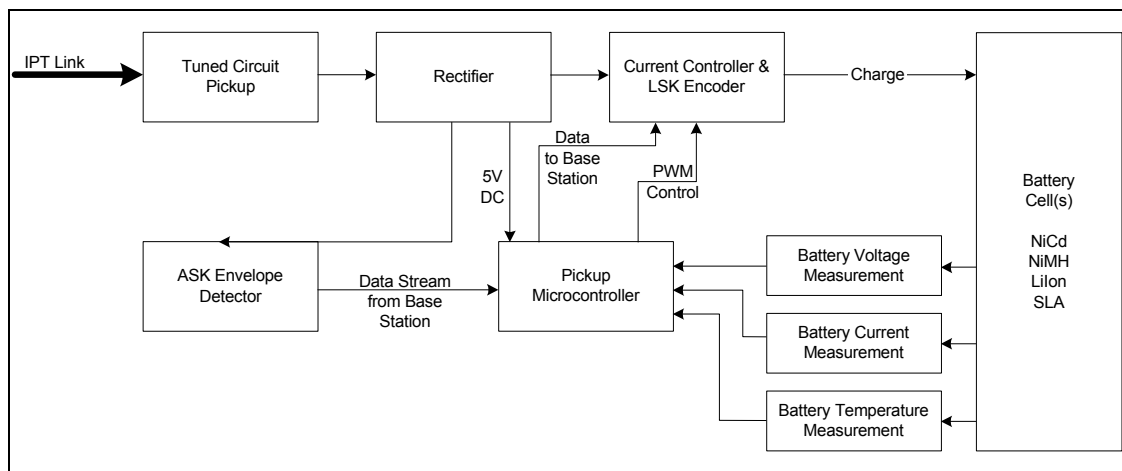


Figure 3.3: Pickup functional block diagram.

The design illustrates a modular approach. In many cases specific functional blocks (e.g. the base station communication encoder) could be replaced or removed without affecting the remainder of the system. This allows the design to be refined or altered with less effort.

### 3.2. Control

The design decision to have microcontrollers in both the base station and pickup circuits was complex. If there was no processor in the pickup the circuit could have been much simpler and the communications would not be necessary. Without a processor the ability to control the charging current to the battery would be very limited and there would be no way to measure battery and charging parameters, which is required for efficient and safe charging, especially for different battery types.

The base station microcontroller is required for the safe starting and stopping of the IPT system. This is because the IPT system uses a method called Zero Voltage Switching, which has very specific startup and shutdown requirements (see Section 4.1.2.3). A number of advantages occur by using this microcontroller to control the battery charging. It allows a user to monitor the system from a PC and it can increase or reduce the power supplied to the circuit depending on the charging requirements of connected pickups to save energy. In addition, the pickup control software can be both simpler and the same for any type of battery.

### **3.2.1. Component Selection**

#### **3.2.1.1. Pickup Microcontroller**

The microcontroller selected for use in the pickup was the Atmel ATmega8L, an 8-bit microcontroller from the Atmel AVR series. The primary requirements for the pickup microcontroller were:

- 3 channels of analogue to digital conversion for measurements.
- 1 USART channel for communication with the base station.
- 1 PWM output for controlling charge current/voltage.
- Relatively low cost (less than US\$5.00)
- In-circuit programmable

The ATmega8L meets all these requirements, and also features an on-chip 8MHz oscillator, operates from a 2.7V-5.5V power supply, and has built-in brownout detection. Another advantage is that the university owns development tools for the ATmega8L and the author has experience with other AVR series microcontrollers.

#### **3.2.1.2. Base Station Microcontroller**

The microcontroller selected for use in the base station was the Renesas (formerly Mitsubishi) M16C/62. The primary requirements for the base station microcontroller were:

- 1 high-speed timer for controlling the Buck converter.
- 1 channel of digital to analogue conversion for controlling the Buck converter.
- 2 USART channels for communication with the pickups and a PC.
- Several Input-Output channels for controlling circuit components.

The Renesas M16C/62 was selected as the base station microcontroller primarily because the university has the component and associated development tools and the author has previous experience working with this microcontroller. It is a powerful 16MHz 16-bit microprocessor with; 20KB of onboard RAM, 256KB of Flash ROM, 3 USARTs and 5 timers with PWM. It is also relatively low cost. Development tools include a C compiler with standard libraries allowing much simpler development and debugging.

### **3.2.2. Base Station Software Implementation**

The base station software was written in ANSI C. This meant implementation was much easier than would have been possible using assembly language, and is portable to most popular microcontrollers. Another advantage was that much of the core processing could be developed and tested on a PC, using the Microsoft Visual C++ 6.0 compiler. After the operation of the software had been verified, the code was recompiled with the Renesas NC30 C compiler, allowing it to be used on the M16 microcontroller.

The UART connected to the IPT communications channel uses an interrupt for reception. Data is added to a buffer in the interrupt and is processed later when the microcontroller has free time. A timer interrupt operating at 100Hz allows the microcontroller to maintain an elapsed time clock, which means timed battery charging operations can occur.

Debugging utilises the C Standard Input-Output functions, which write to a separate UART on the M16. This allows complex information to be written to a connected PC with minimal programming effort. Debugging occurs at a number of different levels and only those selected will actually appear on the output. This debugging channel also provides data to the PC User Interface with updates on battery charging status.

The simplified flowchart shown in Figure 3.4 describes the core operations of the Base Station software.



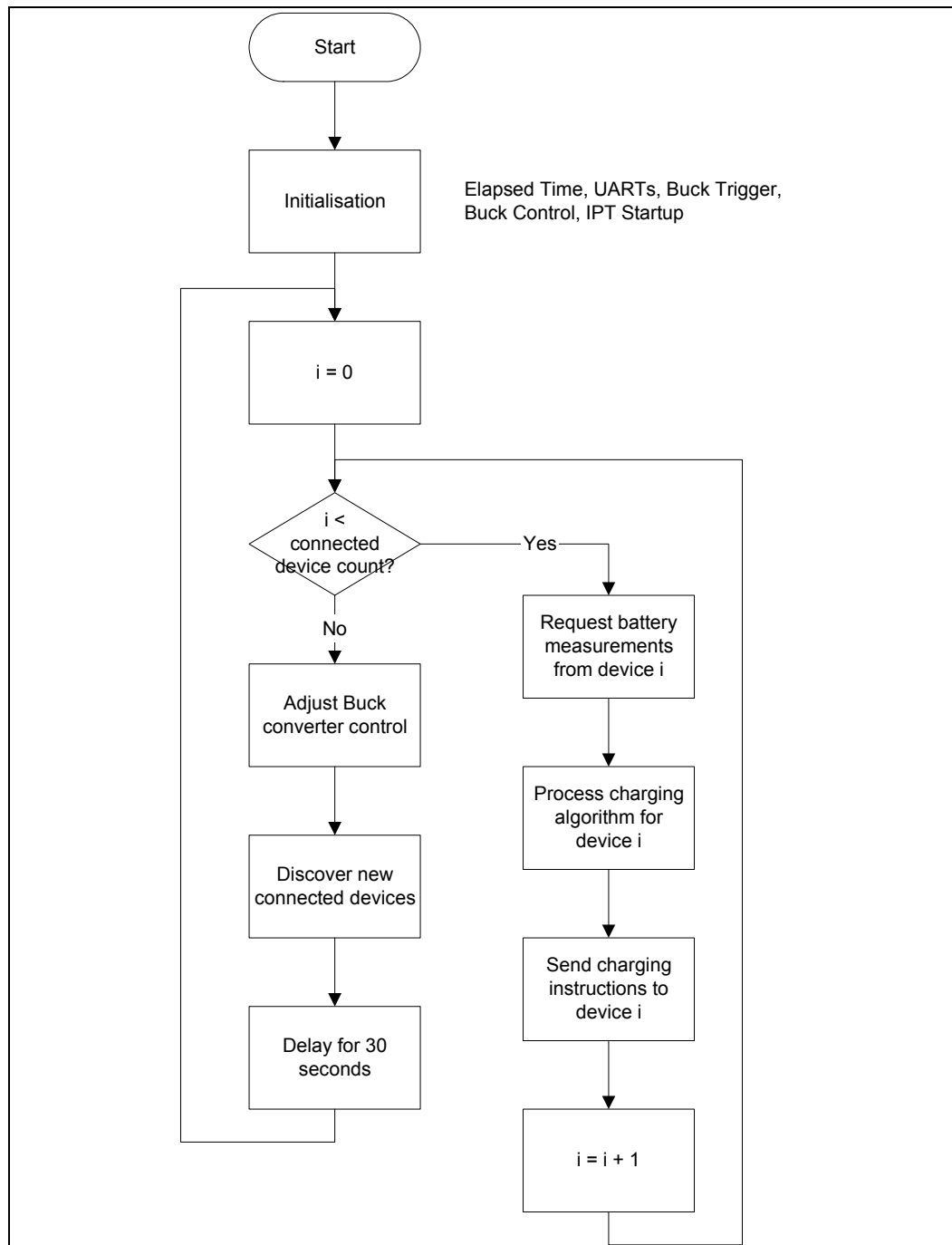


Figure 3.4: Simplified flowchart of the Base Station software.

### 3.2.3. Pickup Software Implementation

The pickup software was written in ANSI C, and compiled using the CodeVision C compiler for the AVR series microcontrollers. Because of the design of the communications protocol code, much of it could be reused verbatim or with minor changes from the M16 implementation.

The Atmega8L software implementation is described by the simplified flowchart in Figure 3.5. As for the M16, an interrupt on the IPT channel UART adds data to a buffer for later processing. A software UART (written in assembly language) was

implemented to allow debugging by sending data to a PC, since the Atmega8L has a single hardware UART.

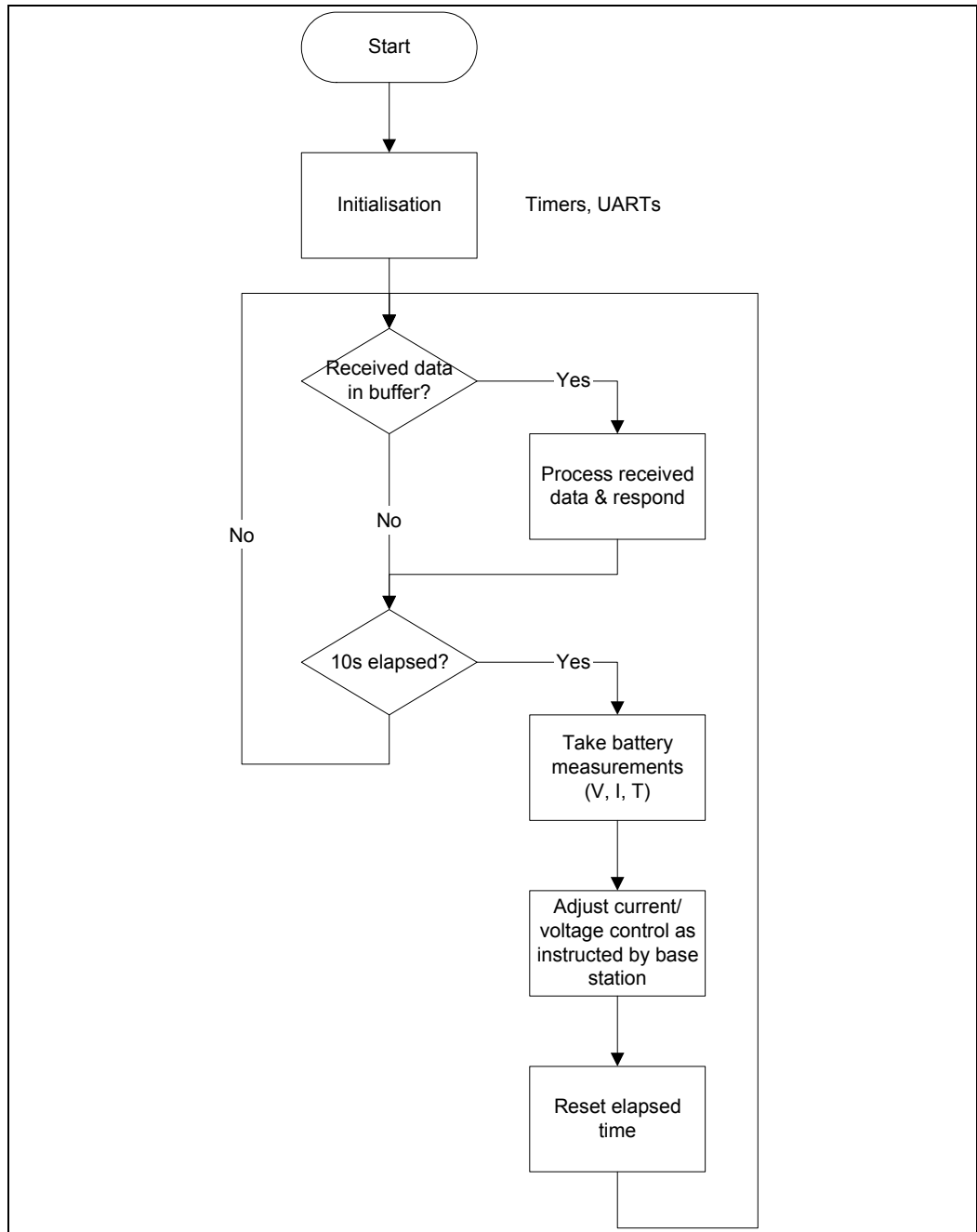


Figure 3.5: Simplified flowchart of the pickup software.

## 4. Inductive Power Transfer

For an overview of the underlying concepts behind IPT please refer to Section 2.1. This section discusses the design of the IPT components for the battery charger project.

### 4.1. Base Station Design

This system has been simulated using the PSpice tool at a number of operating frequencies up to 1MHz. However, at these high frequencies the PSpice models became less realistic. In addition other parameters that cannot easily be simulated such as parasitic capacitance and inductance from circuit board tracks have a significant impact on the operation of an actual circuit. For these reasons the operating frequency of the IPT system was set at 85-90 kHz which is still higher than the typical operating frequency of an IPT system at 10-40 kHz.

#### 4.1.1. Power Supply

A Buck converter is used to control the input voltage to the resonant converter to a maximum of 30V DC. Since the open circuit voltage of the pickup is directly proportional to the input voltage of the resonant converter the Buck converter can be used to control the power delivered to the pickups. This is utilised to adjust the stable power delivered to the pickups as well as to modulate communications from the base station to the pickups. When the input voltage to the resonant tank changes suddenly the system can become unstable. The Buck converter smoothes any changes in input voltage, which prevents this situation.

The base station microcontroller provides both a 85kHz trigger and a 0-5V analogue signal, that are converted into a high frequency pulse-width modulated signal by a 555 timer IC. This is then fed into an optocoupler which uses an isolated power supply to drive the gate of the MOSFET. The operating frequency of the Buck converter is 85kHz, which is limited by the bandwidth of the optocoupler. A schematic of the Buck converter is shown in Figure 4.1.

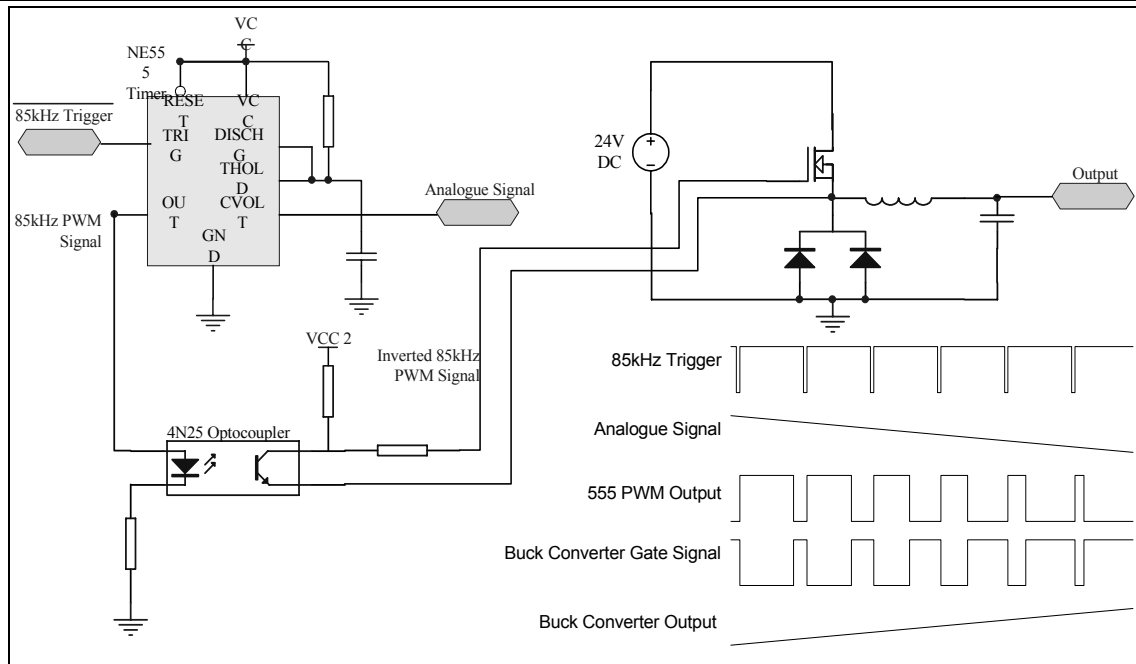


Figure 4.1: Schematic and operation of the Buck converter.

#### 4.1.2. Resonant Converter

The resonant converter has a nominal input of 24V DC. It produces a high frequency sinusoidal output to the air gap which comprises the IPT link with the pickup circuit. The simplified schematic in Figure 4.2 shows the fundamental circuit design using a current fed, half-bridge topology to produce a sine wave with low distortion and minimal electromagnetic interference (EMI) issues.

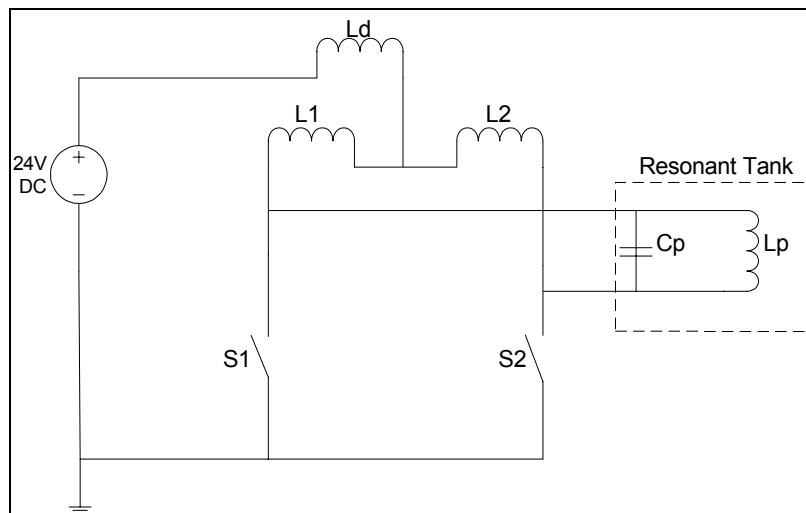


Figure 4.2: Simplified schematic of Base Station.

MOSFETs S1 and S2 are alternately on providing a sinusoidal AC waveform at the input to the resonant tank at its natural frequency when powered by a DC input voltage. MOSFETs are the most suitable switching devices as they can operate at high frequencies and are compact in size.

#### 4.1.2.1. Split Winding Inductor

The split winding inductor (L1/L2) gives a square wave to the resonant tank by splitting the current. Both L1 and L2 need to be at least 10 times the value of Lp for stability. A current source is required and Ld is a DC inductor which provides this. Practically, the leakage inductance from the split winding inductor (L1/L2) implements Ld in the design. By using a split winding inductor with a low coupling coefficient a larger value of Ld is obtained.

#### 4.1.2.2. Resonant Tank

The alternate switching of MOSFETs S1 and S2 provides an AC sine wave as the input to the resonant converter. This is illustrated in Figure 4.3. The peak voltage across the primary inductor is directly proportional to the input voltage as described by Equation 4.1.

$$\hat{V}_{\text{tank}} = \pi V_d$$

Equation 4.1

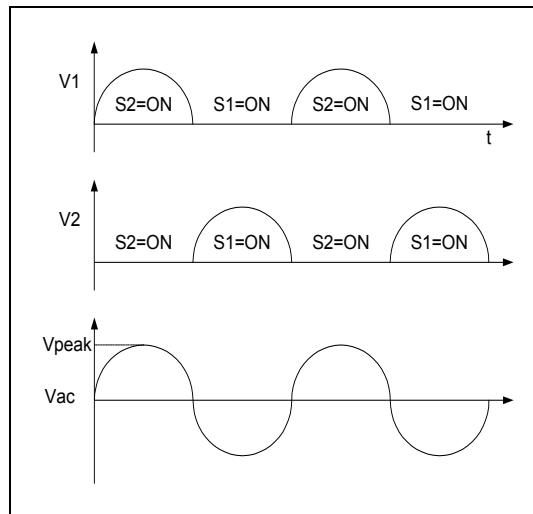


Figure 4.3: Graphs of the switching operation of the resonant converter. V1 and V2 are the voltages across MOSFETs S1 and S2 respectively. Vac is the voltage across the output of the resonant converter.

The resonant tank operates at a natural frequency described by Equation 4.2 after energy enters it. Because of the Zero Voltage Switching design (Section 4.1.2.3) the MOSFETs will also switch at the same frequency.

$$f_0 = \frac{1}{2\pi\sqrt{L_p C_p}}$$

Equation 4.2

### 4.1.2.3. Zero Voltage Switching

A technique known as Zero Voltage Switching (ZVS) has been employed. Using a simple circuit consisting of a comparator and some discrete logic, shown in Figure 4.4, the MOSFETs are switched at the point when the output voltage of the resonant tank is zero. Table 4.1 shows how the logic operates during normal operation and at startup (See Section 4.1.2.4 below).

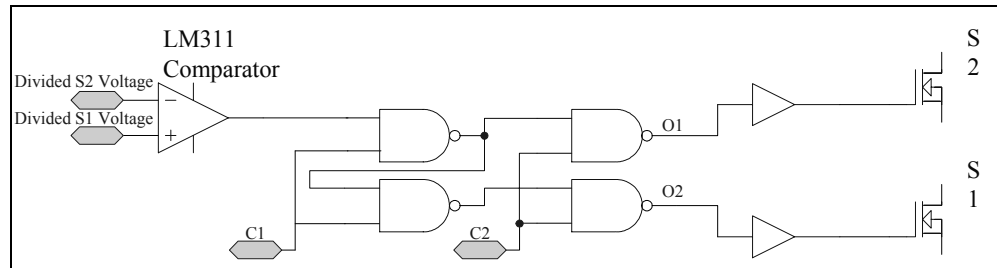


Figure 4.4: Simplified schematic of the Zero Voltage Switching circuit.

Micro controller signals		Comparator output	Quad NAND IC output		Operation Mode
C1	C2		O1	O2	
0	0	X	1	1	Off
0	1	X	0	0	Start-up
1	1	1	1	0	Normal
1	1	0	0	1	Normal

Table 4.1: Control signals and operation of the Zero Voltage switching logic.

In a non-ZVS circuit when switching happens there is a finite amount of time between the switch opening and the current reducing to zero as the voltage increases. This causes; power losses, increased electromagnetic interference, and stress on components. ZVS mitigates these problems and also allows the resonant tank to operate at its natural frequency (which can change with different loads).

### 4.1.2.4. Start-up and Shutdown

At start-up and shutdown additional control is required when using ZVS which is provided by the base station microcontroller. When the power supply is turned on there is no energy in the resonant tank and ergo no zero voltage crossings to detect. The MOSFETs must both be switched on for a short period to allow enough energy to build up in the split winding inductor (L1/L2) so a zero voltage crossing is generated.

The initial current is described by Equation 4.3. In the design, the start-up time has been set at 4µs, to allow sufficient energy to build up without damaging the components.

$$I_d = \frac{V_d}{L_d} t$$

Equation 4.3

When the power supply is turned off the MOSFETs must keep switching for several milliseconds to allow the energy from the resonant tank to dissipate slowly. Without this turn-off period a large voltage spike would occur as the resonant tank becomes open-circuit which will damage components. In the design, the addition of the Buck converter allows energy to dissipate naturally because of its output capacitance.

## 4.2. Battery Pickup Design

The IPT components of the pickup include a tuned circuit and a full wave rectifier. A simplified schematic is shown in Figure 4.5.

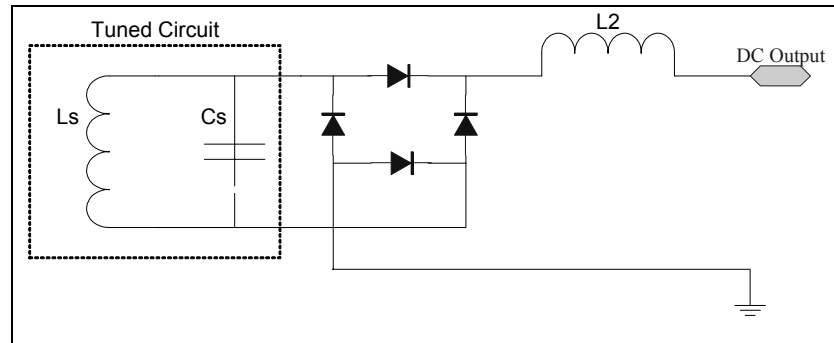


Figure 4.5: Simplified schematic of the battery pickup design.

The tuned circuit has the same natural frequency as the resonant tank at the base station. Because of the high operating frequency the size of the components ( $L_s$  and  $C_s$ ) can be reduced significantly.

The rectifier circuit converts the AC waveform into a DC voltage which is regulated to provide power to the pickup microcontroller and other discrete devices as well as powering the Boost converter used to control current to the battery.

## 4.3. Results and Performance

### 4.3.1. Resonant Converter

The actual parameters of the resonant converter matched the design values as shown in Table 4.2 below. Figure 4.6 shows the operation of the Resonant Converter with measurements to show the effect of Zero Voltage Switching. The voltage spikes at the switching points could be caused by stray inductances or delays in the control circuitry. However, these are still much less than would be expected in a forced switching design.

Parameter	Expected Value	Actual Value
Operating Frequency	88 kHz	87 kHz
DC Supply Voltage	24 V	24 V
Primary Tank Inductance	16 $\mu$ H	15.9 $\mu$ H
Primary Tank Capacitance	200 nF	200 nF
DC Leakage Inductance	0.4 mH	0.4 mH
Split Winding Inductance	1.0 mH	1.0 mH
Primary Tank Voltage	75.36 V <sub>PEAK</sub>	76 V <sub>PEAK</sub>
Primary Tank Current	9.15 A <sub>PEAK</sub>	8.74 A <sub>PEAK</sub>
Initial Tank Current	0.24 A	-
MOSFET Startup Time	4 $\mu$ s	4 $\mu$ s

Table 4.2: Comparison of actual and expected parameter values for Resonant Converter.

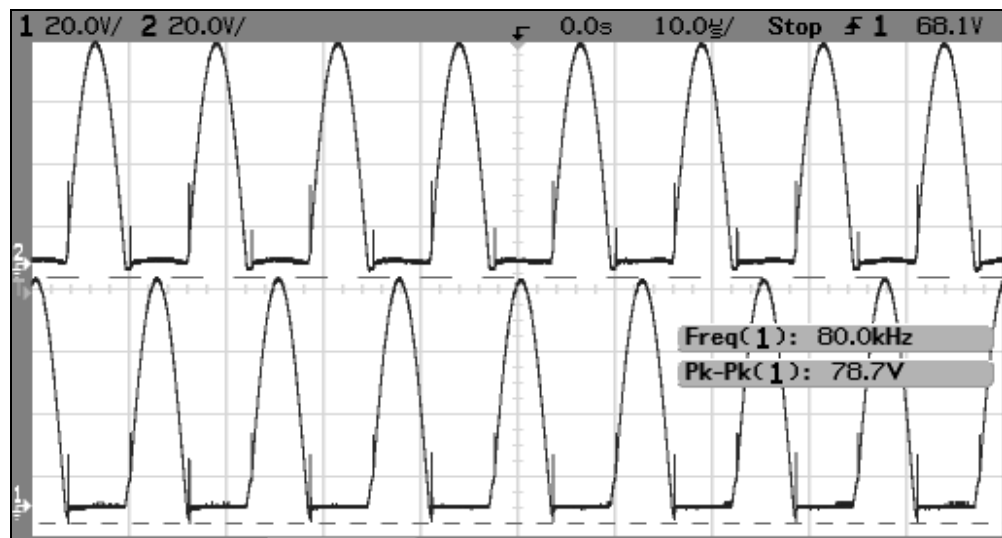


Figure 4.6: Oscilloscope capture of the MOSFET switching in the resonant converter.

#### 4.3.2. Pickup

The parameters for the IPT pickup circuit are shown in Table 4.3. The maximum power transfer is 16.1W into a passive load, suitable for the battery charging application.

Parameter	Value
Tuned Frequency	84.8 kHz
Secondary Inductance	0.8 $\mu$ H
Secondary Capacitance	4.4 $\mu$ F
Secondary Quality Factor (2 $\Omega$ load)	4.7
Secondary Open Circuit Voltage	8.1 V <sub>RMS</sub>
Secondary Short Circuit Current	1.99 A <sub>RMS</sub>
Maximum Power Transfer	16.1 W

Table 4.3: Parameter values for the pickup circuit.



### 4.3.3. Power Efficiency

The power transfer efficiency was measured with different loads on the pickup. The loads used were passive, as batteries present a varying load that is difficult to measure. The results are shown in Figure 4.7.

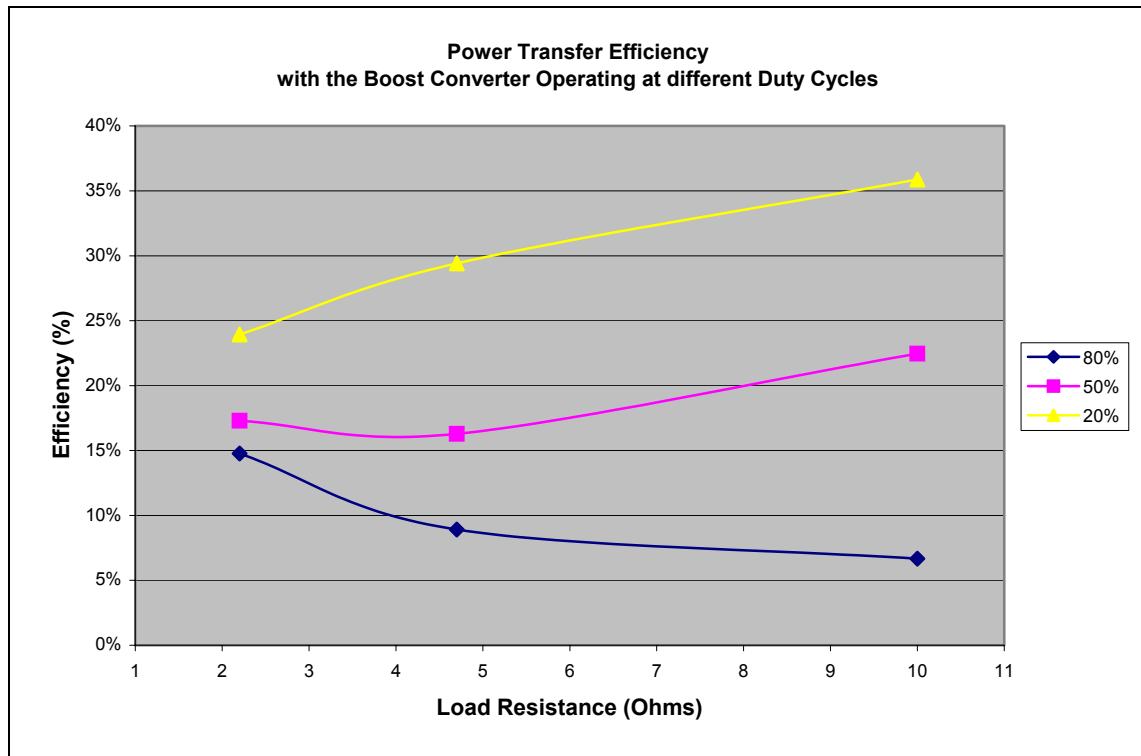


Figure 4.7: Power transfer efficiency for the system under different passive loads, with the pickup Boost converter operating at several duty cycles.

The maximum efficiency is 36%, delivered to a 10Ω load with the Boost converter at 20% duty cycle. This figure is typical for an IPT system. Generally an increase in operating frequency is associated with a drop in efficiency due to increased switching losses. One method to increase efficiency would be to replace the Buck converter on the primary side with a more efficient means of power control.

### 4.4. High Frequency Operation

One of the project aims was to investigate the operation of an IPT system at high frequencies. While the operating frequency (85kHz) is higher than typical IPT systems (10-40kHz), there were a number of issues that arose when increasing the frequency.

As the operating frequency increases, so does the quality factor (Q) and the power transfer capability. This is illustrated by Equation 4.4 and Equation 4.5 below.

$$Q_2 = \omega C_2 R_2$$

Equation 4.4

$$P_2 = \frac{\omega I_1^2 M^2 Q_2}{L_2}$$

Equation 4.5

As the quality factor increases, the pickup circuit tuning needs to be much more accurate to pick up full power from the IPT channel. Because of this difficulty there is often less power transfer at high frequencies due to imperfect tuning or tuning drift. One solutions would be the ability to dynamically re-tune the pickup to compensate for temperature and changes in the operating frequency.

Another observation was that stability decreases with increasing frequency. This could be caused by parasitic capacitances and inductances within the circuit that are difficult to model. At low frequencies they have little effect but become more relevant as the operating frequency increases.

## 5. Communications

Communications utilising the same inductive channel used for power transfer are appealing for a number of reasons. The cost of the additional hardware components used for communication is small compared with that of the IPT system.

While adding radio or Infrared communications is easy it is likely to be both more expensive as well as increasing the complexity and potential for interference.

Combined power and communications contact-less channels have been applied in medical applications, as implantable biotelemeters and the more common RFID tags used in industry. These applications typically have very power requirements of less than 100mW and operate at frequencies of several MHz [4-6]. Many implementations only support one-way communication.

By applying the techniques used in the medical telemeters to the IPT system the aim was to implement a bidirectional communications channel concurrently with the power transfer from base station to pickups. It was necessary for the digital communications signal to be modulated onto the power (carrier) signal between the base station and pickups. Due to the modulation techniques chosen the communication was limited to half duplex, meaning only one party can transmit at a time.

### 5.1. Primary to Secondary

Because the IPT system is controlled from the primary side, there are more options available for modulation of the data signal onto the carrier signal. The options considered were:

- Phase shift keying involves adjusting the phase of the IPT signal with data with little-to-no power loss. While this may be an effective method to explore for future development it requires much more complex modulation and demodulation circuits, and the performance of the IPT system and reverse communications may be affected significantly.

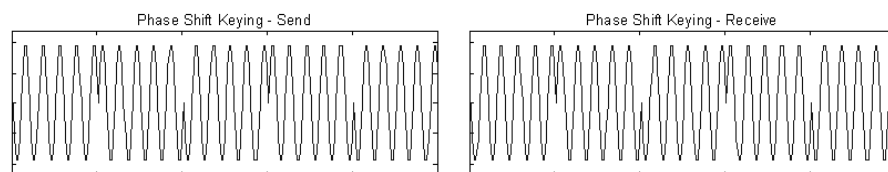


Figure 5.1: Sending and receiving a Phase Shift Keying modulated signal.

- Frequency shift keying involves changing the operating frequency of the IPT link with data. This is achieved by switching additional capacitance into and out of the resonant tank, effectively de-tuning the pickup. This results in a change in amplitude detectable on the secondary side with a loss of power. This method requires a high speed, high voltage AC switch in the resonant tank.

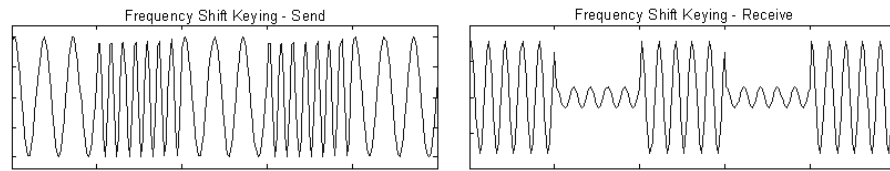


Figure 5.2: Sending and receiving a Frequency Shift Keying modulated signal.

- Amplitude shift keying modulates the signal by adjusting the input voltage to the IPT system with data. This results in an amplitude change detectable on the secondary side, with loss of power. This is simple to implement but is limited to fairly low data rates because the energy stored in the resonant tank smooths changes.

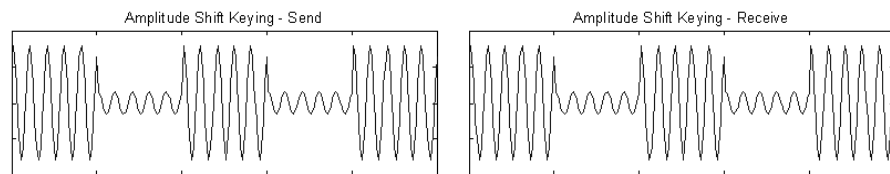


Figure 5.3: Sending and receiving an Amplitude Shift Keying modulated signal

The method implemented was amplitude shift keying, due primarily to its simplicity. Changing the input voltage is performed by a Buck converter which allowed the system to be optimised easily. The Buck converter is also used for adjusting the input voltage to increase the power transfer of the system for large loads.

The modulated signal is detected on the secondary side using an AM envelope detector as shown in Figure 5.4 below.

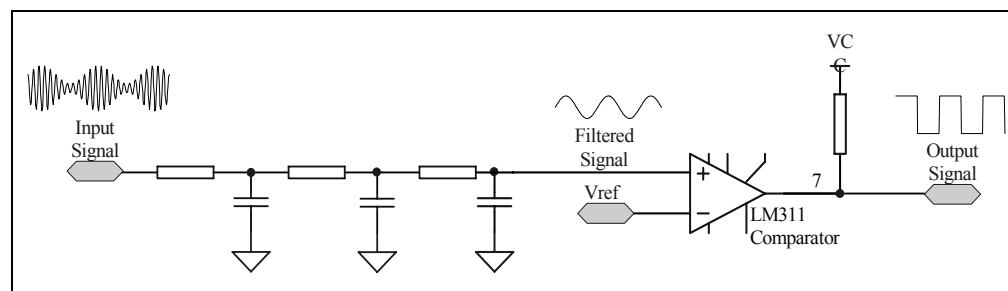


Figure 5.4: Simplified schematic showing the operation of the envelope detector.

## 5.2. Secondary to Primary

In every IPT system the pickup reflects a voltage back to the primary side. This voltage depends on the size of the load and the relative sizes of the primary and secondary inductors, as described in Equation 5.1, where  $Z_s$  is the load impedance on the secondary.

$$|V_r| = \frac{I_1 \omega^2 M^2}{Z_s} \approx \frac{M^2 I_1 R_2}{L_2^2}$$

Equation 5.1

By varying the effective load, the pickup can communicate with the base station. This technique is known as Load Shift Keying (LSK). On the primary side a simple AM envelope detector circuit can detect the change in reflected voltage, similar to that shown in Figure 5.4.

For LSK to be effective, the resonant tank and pickup must be tuned and have a lower primary to secondary inductor ratio than normal. This is a trade-off between the stability of the circuit and the modulation available for communications.

In the design for the charger LSK is implemented using the Boost converter already on the pickup (see Section 6.1.2). By turning this completely off or on the reflected impedance changes enough to be detected on the primary side.

## 5.3. Envelope Detection

On the primary and secondary sides, low pass filters are used to extract the data signal from the underlying carrier frequency. RC filters have been implemented to reduce complexity.

On the base station side, the voltage across one of the MOSFETs is divided. This is then passed through a third order low pass RC filter, amplified, re-biased and input to a comparator. The output of the comparator produces a 0-5V signal matching the data signal and is passed to a UART on the M16 microcontroller.

On the pickup side, the voltage across a sense resistor in series with the battery is passed through a third order low pass RC filter, amplified, re-biased and input to a comparator. The output of the comparator is a 0-5V signal matching the data signal and is passed to the UART on the AVR microcontroller.

## 5.4. Protocol Design

Because of the general unreliability of wireless data transmission (especially when combined with power transfer) it was important to ensure that any errors could be detected in software. A robust protocol, supporting multiple devices and including error detection and device discovery, was implemented.

The link-layer interfaces for the channel are standard UART ports. This simplifies implementation (as nearly all microcontrollers have UARTs) and allows easy substitution of wires, infrared, or radio as alternate physical methods. UARTs are active-low devices and are configured to use an 11-bit packet. This consists of one start bit, eight data bits, one even parity bit and one stop bit.

### 5.4.1. Network Topology

A master-slave network was considered the most appropriate for the battery charger model, as pickups (slaves) would only be communicating with the base station (master). The master device controls all communication, initiating every request, and waiting for a response from the slave.

Each connected device has an ID number that is automatically allocated by the device discovery process (see Appendix A). ID 0 is unique – it is the default ID for unconnected devices and is a broadcast ID where all devices process any received messages.

A message is resent 4 times if a packet requires a response but the master does not receive it. After 4 retries the device is sent a message to change its ID to 0 and the master removes the device record. Separately, if a slave device has had no communication from the master in 3 minutes it changes its ID to 0 so it can be rediscovered.

### 5.4.2. Packet Format

The packet format employed for communication has been designed to be flexible, allowing for future expansion. Having a variable packet size minimizes the communication, which is important as communication reduces the power transfer in the inductive channel. The packet format is shown in Figure 5.5 and each field is explained in detail below.

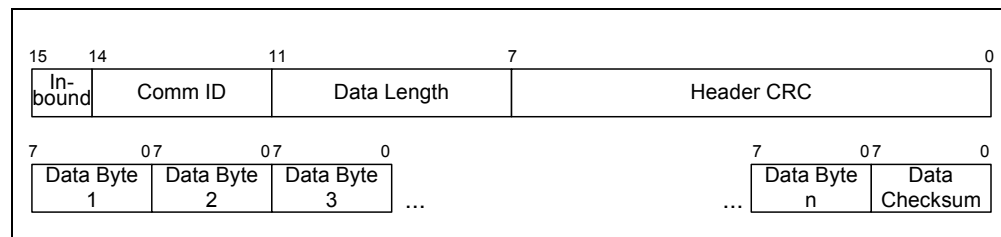


Figure 5.5: Communications data packet format.

- Header – 2 bytes
  - Inbound flag – specifies whether a packet is destined for the master from the slave with the specified ID (=1) or from the master to the specified slave (=0).
  - Communication ID – a unique number allocated to a device during device discovery. ID 0 is the default address and is also a broadcast address.
  - Data Length – the length of the following data packet. This is specified in bytes from 0 to 15. The data checksum is not included in this count. If a data length of 0 is specified there is no data component to the packet or data checksum.
  - Header Checksum – an 8-bit CRC allows the header to be verified before the rest of the message is received. See Appendix B for a description of the CRC algorithm used.

- Data – 1-15 bytes
  - Data Bytes – the data to send. The number of data bytes is stated in the Data Length field in the header.
  - Data Checksum – an 8-bit CRC allows the data to be verified. The data checksum uses a different ‘seed’ from the header so 1 byte data packets cannot be incorrectly identified as headers. See Appendix B for a description of the CRC algorithm used.

Generally, the first data byte contains a command code which determines the purpose of the packet. Many commands require a response or acknowledgment from the battery device. See Appendix D for a complete description of the implemented commands and packets.

### 5.4.3. Device Discovery

The communication protocol specifies a method of finding new devices connected to the system, without disrupting normal communications. This method is simple but can scale to a large number of devices. The flow chart in Appendix A illustrates how the procedure operates. Device discovery is initiated by the master once every 30 seconds, as well as immediately after power-on.

## 5.5. Results and Performance

The final communication speed in either direction was set at 300bps (150Hz). While this is lower than originally designed it has a small error rate under any load conditions and is sufficient for the battery charging application. Since amplitude modulation is used, the longer 7ms pulses result in increased power losses from communication than in the original design.

The error rate was determined by sending a large amount of data across the link, and counting the number of bit errors received. Parity and frame errors accounted for nearly all errors recorded. The bit error rates recorded for forward communication are shown in Table 5.1. The errors are higher for smaller packets due to the slow initial response of the resonant converter and Buck converter to changes.

Charge Current	Packet Size		
	1 byte	7 bytes	10 bytes
Low	0.13%	0.01%	0.00%
Medium	0.17%	0.01%	0.12%
High	0.04%	0.00%	0.00%

Table 5.1: Forward communications bit error rates.

Reverse communications from the pickup to the primary also perform well at 300bps. The results are shown in Table 5.2. The increased noise is primarily due to the 85kHz carrier signal that was not perfectly filtered due to its frequency proximity to the data signal.

Charge Current	Packet Size		
	1 byte	7 bytes	10 bytes
Low	0.30%	0.33%	0.31%
Medium	0.14%	0.30%	0.26%
High	0.18%	0.31%	0.32%

Table 5.2: Reverse communication bit error rates.

The modulation index of the signal onto the IPT power waveform was also measured and the results are shown in Figure 5.6 below. This shows adequate modulation occurred at 10kHz in the reverse direction, while in the forward direction modulation decreased with frequency due to the slow response time of the Buck converter and resonant tank to changes in voltage.

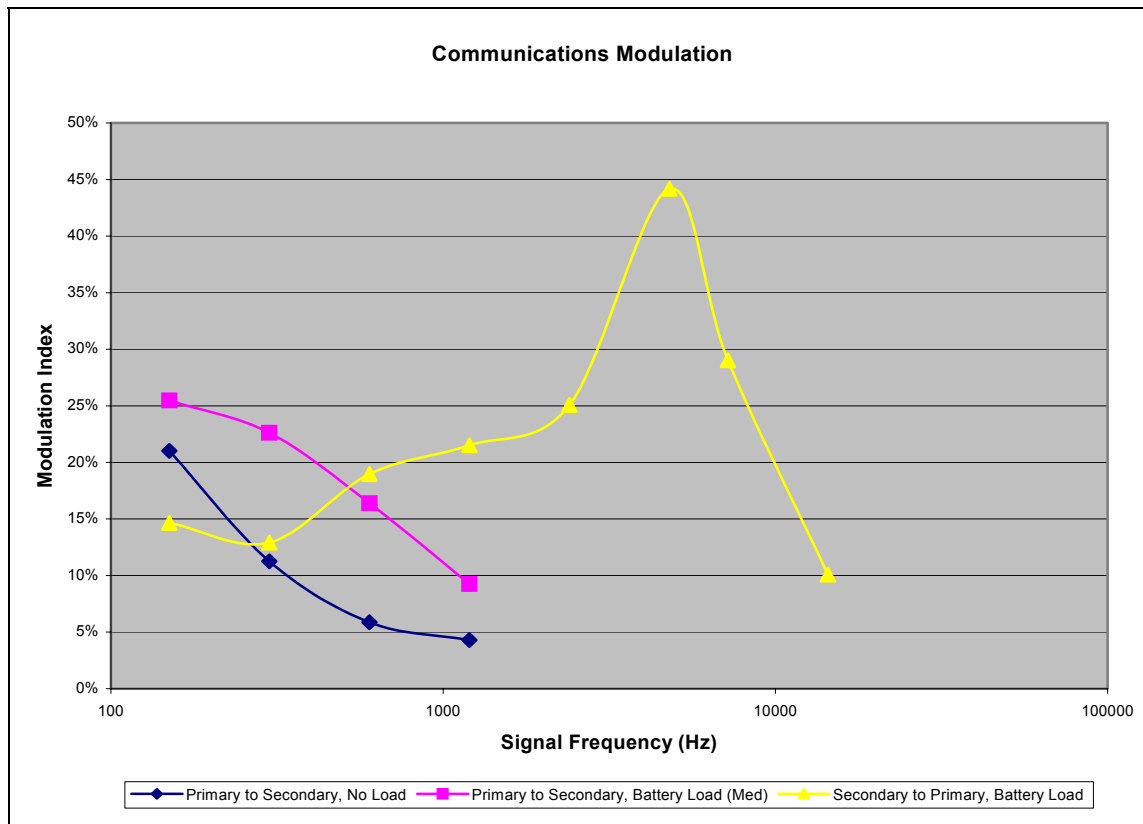


Figure 5.6: Modulation Indexes of the communications at different frequencies.

Two oscilloscope captures shown in Figure 5.7 and Figure 5.8 below indicate the modulation of the data signal onto the carrier and the output of the envelope detection circuits for the forward and reverse directions respectively.



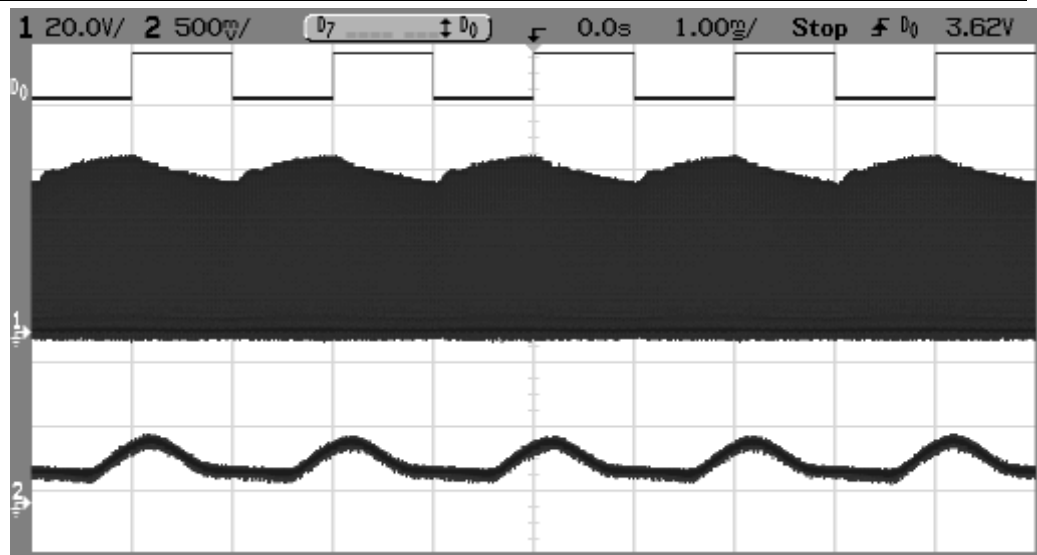


Figure 5.7: Modulation of a 1kHz square wave onto the power waveform from the primary side with the output of the secondary envelope detector.

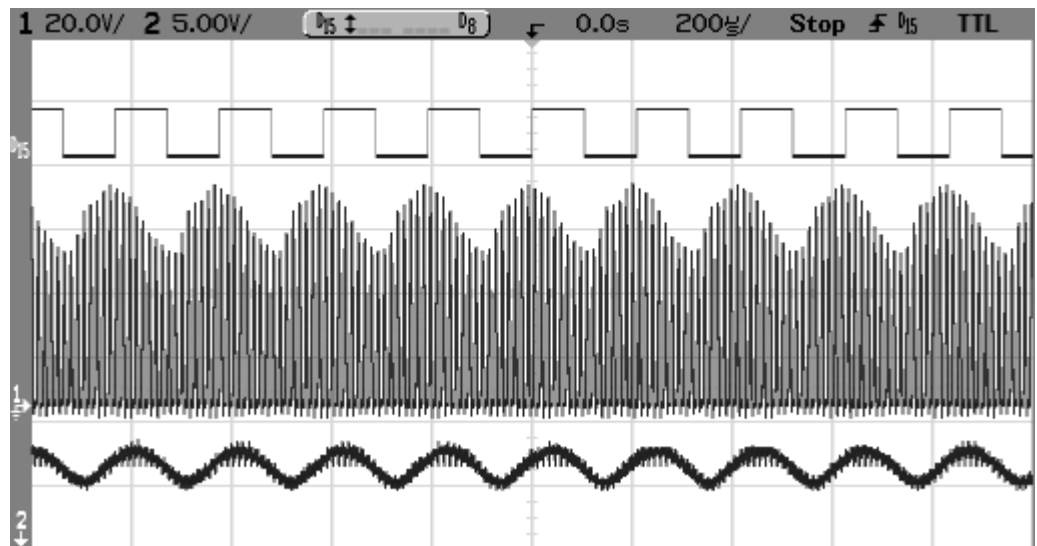


Figure 5.8: Modulation of a 4.8kHz square wave onto the power waveform from the secondary side with the output of the primary envelope detector.

As discussed in Section 7.3, there are a number of ways to improve the performance of the communication system in the future. One method is to replace the RC filter circuits with more complex filters that have better attenuation. The modulation index does not then need to be as high to achieve the same signal to noise ratio, allowing operation at higher frequencies.

## 6. Battery Charging

### 6.1. Charging Control

One of the main goals of the project was to be able to charge multiple batteries concurrently. The charger supports four of the most popular rechargeable batteries.

The battery charging uses a distributed control system. The base station is responsible for executing the charging algorithm for each connected device depending on its type. The pickup takes battery measurements and controls the current and voltage delivered to the battery as instructed by the base station.

#### 6.1.1. Battery Measurements

A number of measurements need to be made during battery charging in order to control the current and voltage and monitor the battery to determine when to switch between fast charge and trickle charge modes. The pickup controller measures the battery voltage, charge current, and battery temperature. Different battery types utilise a combination of measurements to control the charging process.

The measurements are taken using three of the channels of analogue-to-digital conversion (ADC) available on the pickup microcontroller. To ensure accurate ADC measurements, a series of samples are made until the values stabilize, followed by an averaging process. This algorithm is shown in Appendix C.

The charge current is measured across a small sense resistor in series with the battery. The battery voltage is measured across the terminals but this must be done when there is no charge current. Conversely the charge voltage is measured in the same way when charge current is being applied. Most battery packs include a thermistor for measuring the temperature of the cells and this is also monitored. A schematic for the measurement components of the pickup circuit is shown in Figure 6.1 below.

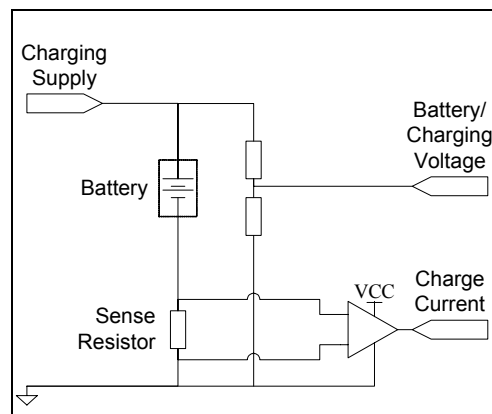


Figure 6.1: Simplified schematic of the battery voltage and charge current measurement circuits.

### 6.1.2. Current and Voltage Control

Charging Li-Ion and SLA batteries requires control of both the current and voltage applied to the battery. In the design a Boost converter is used to regulate the current applied to the battery as shown in Figure 6.2. The Boost converter is controlled by the pickup microcontroller which provides a 0-5V 33kHz pulse width modulated signal. The duty cycle of this signal determines how much current flows to the battery.

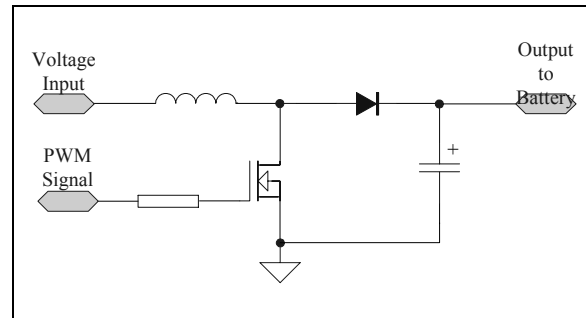


Figure 6.2: Simplified schematic of the Boost converter circuit.

By monitoring both the charging current and the battery voltage with the pickup microcontroller, voltage control over the battery can be maintained. This takes into account that battery charging is a very slow process by electronic standards. Over a number of measurements of the charge voltage, the voltage can be regulated using an iterative process, adjusting the charge current by a small amount and then re-measuring the voltage until the voltage reaches the target value. This process will repeat as the charge current gradually changes, readjusting the system to maintain a constant voltage. Appendix E shows this algorithm in detail.

## 6.2. Battery Technologies

The major types of portable rechargeable battery currently in use are Nickel Cadmium (NiCd), Nickel Metal Hydride (NiMH), Lithium Ion (Li-Ion) and Sealed Lead Acid (SLA). Each is briefly outlined below. All voltages indicated are for a single-cell battery. The term C refers to the rated capacity of the battery (e.g. 1000mAh). [7-11]

### 6.2.1. Nickel Cadmium

Nickel Cadmium (NiCd) batteries were invented in 1899 and have been in production since the early 1960s. These are low cost, convenient, and can be typically used for 500-1000 charge and discharge cycles.

Battery charging is using a constant current of 0.5-1C mA for 1-2 hours followed by trickle charging at 0.05C mA. The transition from fast to trickle charging occurs when the voltage begins to drop after the battery is fully charged. The temperature rise that occurs when the battery is charged can also be used as a backup method.

### 6.2.2. Nickel Metal Hydride

Nickel Metal Hydride (NiMH) batteries were developed in the 1980s. The major advantage is that NiMH batteries provide a higher energy density than NiCd batteries. They are fully compatible with NiCd systems and typically have a life of 500 cycles. They were the predominant battery used in portable applications until the development of the Lithium Ion technology.

Charging of NiMH batteries uses a constant current of 0.5-1C mA for 60-90 minutes, followed by 10-20 hours of trickle charging at 0.04C mA. The transition from fast to trickle charging can be initiated by either the voltage drop or temperature rise techniques.

### 6.2.3. Lithium Ion

The most popular battery technology currently is Lithium Ion (Li-Ion). It provides the highest energy density as well as being lightweight and having a high voltage rating of 3.7V. Li-Ion batteries are currently used in laptops, camcorders, mobile phones and other portable devices. As Li-Ion batteries are less tolerant of over-charging and over-discharging, and can explode or ignite if mistreated, cells are only available to equipment manufacturers, who package them for specific uses and include simple protection circuits into the battery packs.

Li-Ion batteries are charged using the constant voltage/constant current method. Fast charge occurs at a constant current of 1C. When the cell voltage reaches 4.1V the battery is charged at a constant voltage of 4.1V until the current drops below 0.1C mA.

### 6.2.4. Sealed Lead Acid

Sealed Lead Acid (SLA) batteries have been available for over 30 years, and are commonly used in applications where space and weight are not a concern, and cost is important. They are often used for electric chairs, uninterruptible power supplies and as backup batteries in alarm systems.

The SLA battery is charged using a constant current of 0.4C until the voltage reaches 2.4V, then trickle charged at a constant voltage of 2.4V indefinitely.

## 6.3. Results and Performance

The maximum measurement accuracies of the pickup in respect to voltage, charge current and temperature are shown in Table 6.1 below. To counter the natural variation in analogue to digital converter readings 8 samples are taken and their values averaged to reduce anomalies.

Parameter	Range	Maximum Accuracy
Battery Voltage	0 – 6.0 V	6.2 mV
Charge Current	0 – 2.0 A	8.1 mA
Battery Temperature	10 – 125 °C	1.5 °C

Table 6.1: Battery parameters measurement accuracy.

Controlling the charge current to the battery by using the boost converter has an accuracy of ~14mA but this varies depending on the current level and charge status. Because of this the iterative approach used to adjust the charge current

and voltage is appropriate allowing the system to adapt to different charging conditions.

Charging at currents below 150mA can compromise the stability of the system under some circumstances. In general this is not a problem as 90-95% of the battery charge has been restored before the charge current drops below 150mA. However, trickle charging (charging for long periods at typical currents of 50-100mA to restore full battery charge) is not possible with the current design.

Nickel Cadmium batteries suffer from a memory effect meaning they should be fully discharged before being charged. This discharging process is not currently supported by the design, but could be easily developed. Other enhancements including trickle charging and battery type detection are discussed in Section 7.2.

## 7. Future Developments

There are a number of ways to develop this project further in the future. Many of the techniques used could be applied to different applications.

### 7.1. Inductive Power Transfer

By further increasing the operating frequency components can become smaller which is important for all applications but especially consumer electronics. Theoretically, the maximum power transfer of an IPT system increases with frequency. However, the increase in parasitic capacitances, inductances, and switching losses can erode this gain.

It is difficult to tune components at high frequencies and facilities for doing this need to be available. Improving modelling tools such as PSpice to cater better for high frequency IPT systems will also assist with development.

Developing a way to dynamically re-tune an IPT pickup circuit could allow improvements in a number of areas. This dynamic re-tuning could keep the pickup tuned to the primary circuit even under changing conditions.

### 7.2. Battery Charging

To aid in reducing the pickup size, an alternate form of current control could be utilised in order to eliminate the Boost converter in the pickup circuit. One method of achieving this would be for the pickup to dynamically de-tune itself. This would allow the pickup to provide the appropriate current to the battery without a large converter.

Trickle charging at low current levels can cause stability problems in IPT systems because they are effectively very small loads. Again, being able to de-tune the pickup instead of using a small load could resolve this issue.

The ability to determine the type of any connected battery automatically would simplify the system further. This would require the analysis of the charging profiles of a large range of different battery types so a specific type could be identified early in the charging process before the potential for wrong charging decisions arises.

### 7.3. Communications

Communications bandwidth could be improved in a number of ways. By increasing the IPT operating frequency the communications rate should increase correspondingly while maintaining the carrier to signal frequency ratio.

Using a different modulation technique such as frequency shift keying could improve bandwidth in the forward direction. This would be relatively straightforward to implement, by adding another capacitor to the resonant tank which can be switched in and out of the circuit. Frequency shift keying should provide faster response to any change, as the amount of energy in the resonant tank does not have to change.

While phase shift keying may seem to be a better technique (with its small power loss) it could become extremely complex to implement. With bidirectional communication the pickup needs to have a significant effect on the primary circuit. Typically this results in a frequency shift in the primary resonant tank which would not happen in a forced-switching phase shift keying situation. In addition, forced switching increases losses and EMI, which become more important at higher operating frequencies. A hybrid control system consisting of zero voltage detection, phase shift keying, and forced switching may be a possible solution.

By using data encoding techniques from wireless digital communication (e.g. Turbo Coding) the performance of the communication link could be improved. These techniques would allow the channel to work effectively at higher speeds when noise and errors increase.

For devices such as Personal Digital Assistants (PDAs) the charger could be expanded to provide data synchronisation – charge the device at the same time as it synchronises data.

## 8. Conclusions

This report reviews the successful design and implementation of a contactless universal battery charger utilising inductive power transfer (IPT). The charger design consists of a base station and a series of pickups, each connected to a battery. The base station controls the charging process on each pickup simultaneously through the use of a microcontroller.

The IPT design involves a parallel resonant converter, incorporating zero voltage switching to improve efficiency, and a tuned resonant tank. A Buck converter controls the input voltage to the resonant converter and the power delivered to the IPT link. The pickup circuit consists of a tuned circuit matched to the operating frequency and a rectifier. The system delivers a maximum of 16W to a passive load, which is sufficient for the battery charging application. The maximum efficiency was 36%, which is typical for an IPT system.

One of the project goals was to investigate the operation of IPT at high frequencies. The charger design operates at a frequency of 85kHz compared to the 10-40kHz typical operating frequency of an IPT system. Operating at a high frequency has a number of advantages including the reduction in size of reactive components in both the base station and pickups and increased power transfer capacity. However difficulties in tuning the pickup circuit increase dramatically with frequency, along with increased switching losses and reduced stability.

A bidirectional communication system utilising the same inductive link used for power transfer was designed. This uses amplitude shift keying to modulate the signals from the base station to the pickups, implemented using the Buck converter. To communicate from the pickups to the base station, a technique known as load shift keying was used. This effectively changes the load which alters the reflected voltage in the primary resonant tank. A master-slave network topology includes a communications protocol incorporating error detection and device discovery. While adequate modulation was achieved at up to 10kHz, the baud rate was set to 300bps in each direction with a resulting bit error rate of 0.3%.

The base station is controlled using a Renesas M16C microcontroller and is responsible for coordinating all charging and adjusting power delivered to the IPT system. Each pickup also contains an Atmel ATmega8L microcontroller; to measure battery parameters and control the charge voltage and current delivered to the battery.

The rechargeable battery types supported by the charger are Nickel Cadmium, Nickel Metal Hydride, Lithium Ion and Sealed Lead Acid, as these are the most common in portable applications. The charging processes are different for each, with both voltage and current control required. This is implemented using a Boost converter in the pickup and an iterative control algorithm.

Future improvements to the system could include increasing the operating frequency, de-tuning the pickup to control charge current more effectively without needing the Boost converter, and using different modulation and encoding techniques to improve the communications bandwidth.



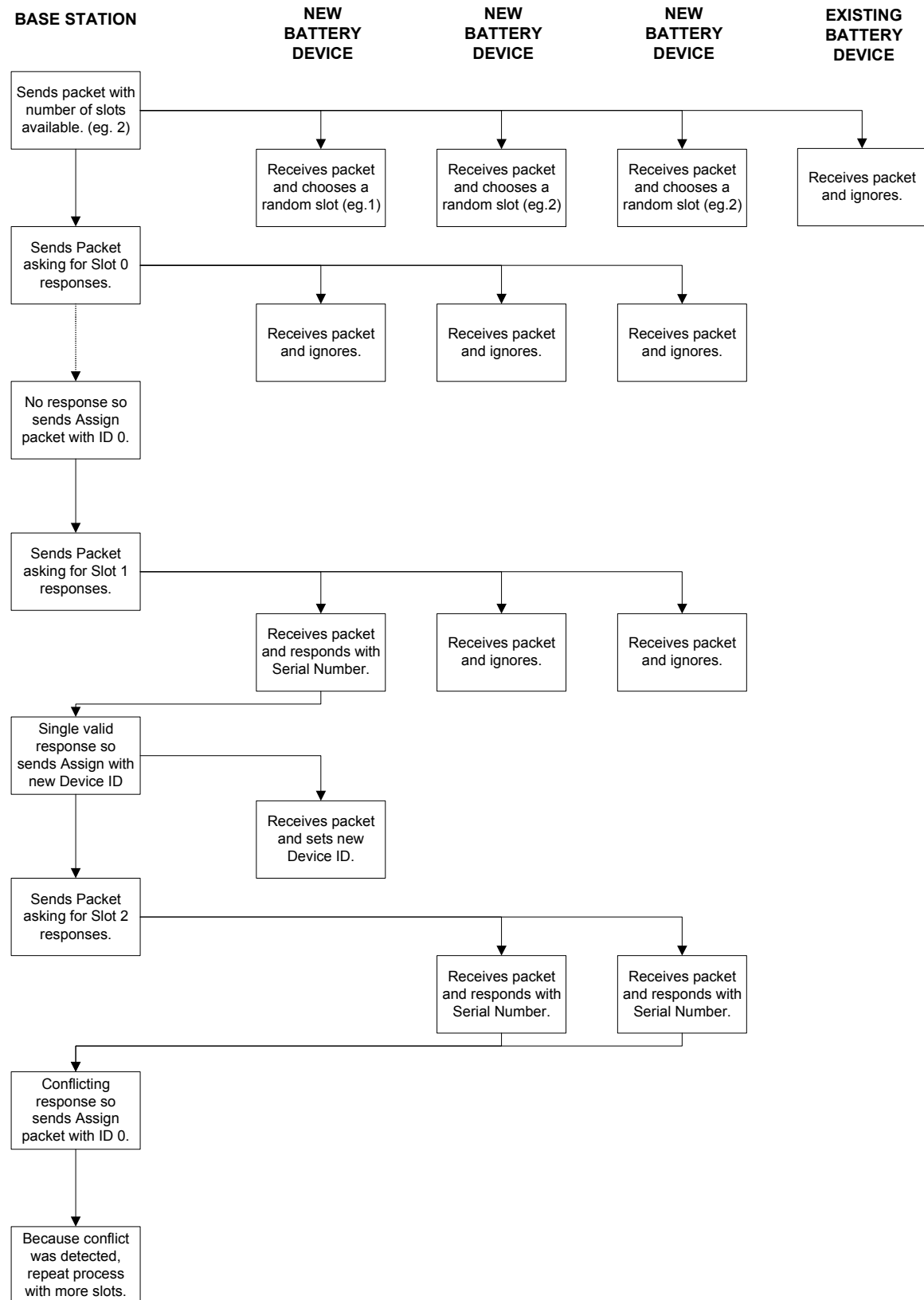
## 9. References

- [1] S. Patel, "Part IV Project: An Automatic Contactless Battery Charger for Robot Power Supplies," Dept. of Electrical and Electronic Engineering, University of Auckland 2002.
- [2] P. Vyas, "Part IV Project: An Automatic Contactless Battery Charger for Robot Power Supplies," Dept. of Electrical and Electronic Engineering, University of Auckland 2002.
- [3] J. T. Boys and A. W. Green, "Inductively Coupled Power Transmission - Concept, Design, and Application," *IPENZ Transactions*, vol. 22, pp. 1-9, 1995.
- [4] Y. Hu, J. Gervais, and M. Sawan, "High Power Efficiency Inductive Link with Full-Duplex Data Communications," PolyStim Neurotechnology Laboratory, Department of Electrical Engineering, Ecole Polytechnique de Montreal.
- [5] Z. Tang, B. Smith, J. H. Schild, and P. Hunter Peckham, "Data Transmission from an Implantable Biotelemetry by Load-Shift Keying Using Circuit Configuration Modulator," *IEEE Transactions on Biomedical Engineering*, vol. 42, pp. 524-528, 1995.
- [6] Y. T. Chuah, P. K. Chan, and L. Siek, "A wireless telemetry system for strain measurement," presented at 2000 Canadian Conference on Electrical and Computer Engineering, 2000.
- [7] "Nickel Cadmium Batteries Technical Handbook," Matsushita Battery and Industrial Co Ltd 2000.
- [8] "Lithium Ion Batteries Technical Handbook," Matsushita Battery and Industrial Co Ltd 2000.
- [9] "Sealed Lead-Acid Batteries Technical Handbook," Matsushita Battery and Industrial Co Ltd 2000.
- [10] "Nickel-Metal Hydride Batteries Technical Handbook," Matsushita Battery and Industrial Co Ltd 2001.
- [11] "Battery Charger for SLA, NiCd, NiMH and Li-Ion Batteries," *Application Note AVR450*: Atmel Corporation, 2002.
- [12] D. Quinz, "Computing a 8-bit CRC or equivalent." Usenet: comp.arch.embedded, 8/11/1998.

## 10. Bibliography

- J. T. Boys, G. A. Covic, and A. W. Green, "Stability and control of Inductively coupled power transfer systems," IEE Proceedings - Electrical Power Applications, vol. 147, 1999.
- R. Coup, Y. T. Lee, C. C. Yu, and J. Y. Kuo, "Engineering Design 3CS Project Two: Infrared Communications," Dept. of Electrical and Electronic Engineering, University of Auckland 2002.
- A. Esser, "Contactless Charging and Communication for Electric Vehicles," in IEEE Industry Applications Magazine, 1995.
- J. Herrmann, "Battery chemistries and charging," in Electronic Products, 2002.
- A. P. Hu, "Selected Resonant Converters for IPT Power Supplies," in Dept. of Electrical and Electronic Engineering: University of Auckland, 2001.
- M. Ryan, "Part IV Project Interim Report: An Inductively Coupled Universal Battery Charger," Dept. of Electrical and Electronic Engineering, University of Auckland 2003.
- O. H. Stielau, J. T. Boys, G. A. Covic, and G. Elliot, "Battery charging using loosely coupled inductive power transfer," presented at Eighth European Conference on Power Electronics and Applications, 1999.

## Appendix A. Device Discovery



## Appendix B. CRC Algorithm

The CRC algorithm is derived from the DOW CRC polynomial. [12] The algorithm is called for each byte to generate a CRC over.

*crc* – existing CRC value. This is used as the seed for the following calculation. To differentiate 2-byte data packets from 2-byte headers, the CRC values are initially set to:

- Header: 0xFF
- Data: 0xAA

*data* – the byte of data to generate the CRC for.

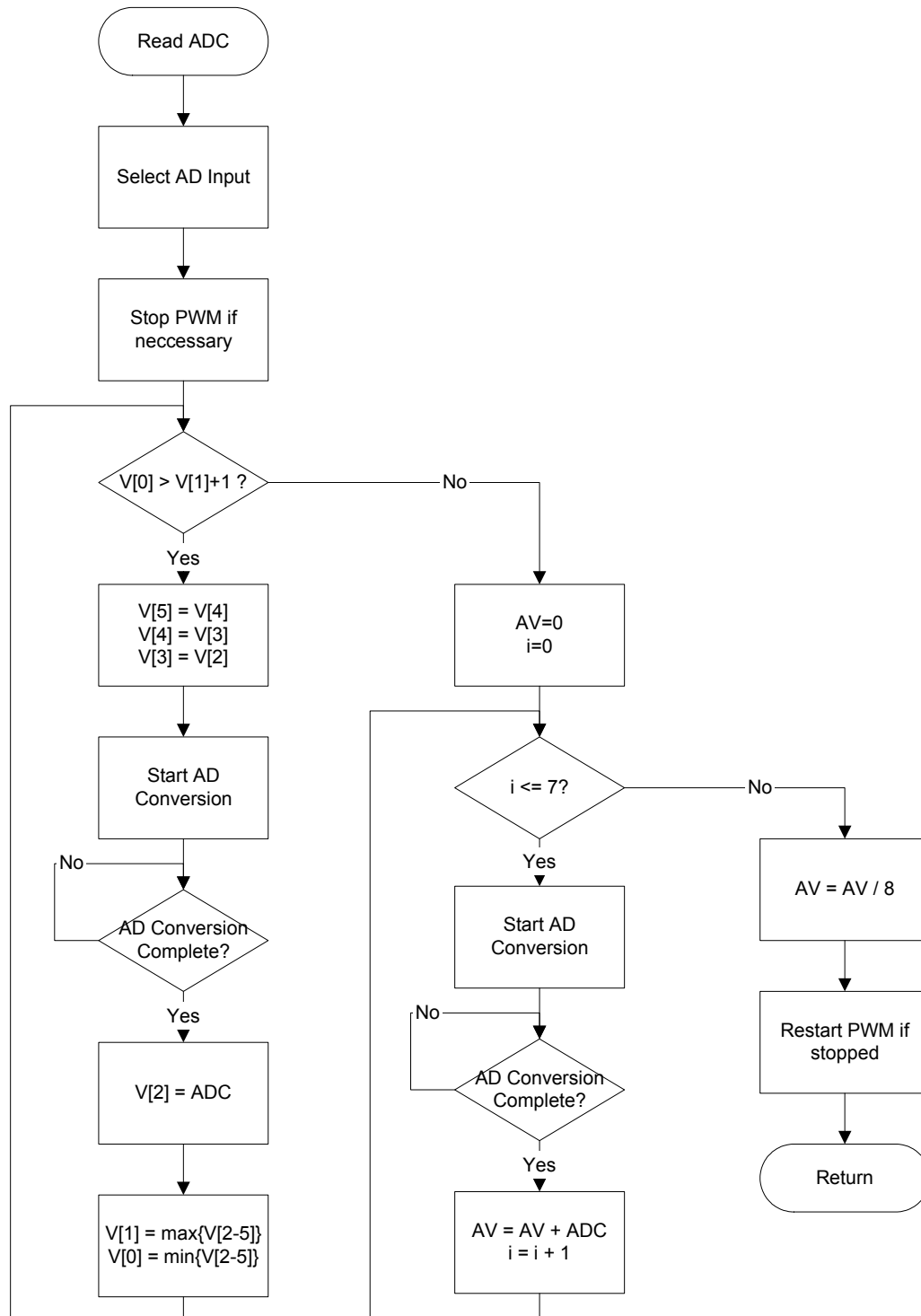
```
for loop = 8 to 1
(
    b = (crc ^ data) & 0x01
    crc = crc >> 1

    if (b != 0)
        crc = crc ^ 0x8C

    data = data >> 1
)
```

## Appendix C. ADC Data Capture Algorithm

A stable reading of the Analogue to Digital Converter (ADC) is required. The following algorithm waits for the ADC to stabilise then takes 8 readings and calculates the average. This algorithm is based on Atmel's recommended procedures. [11]

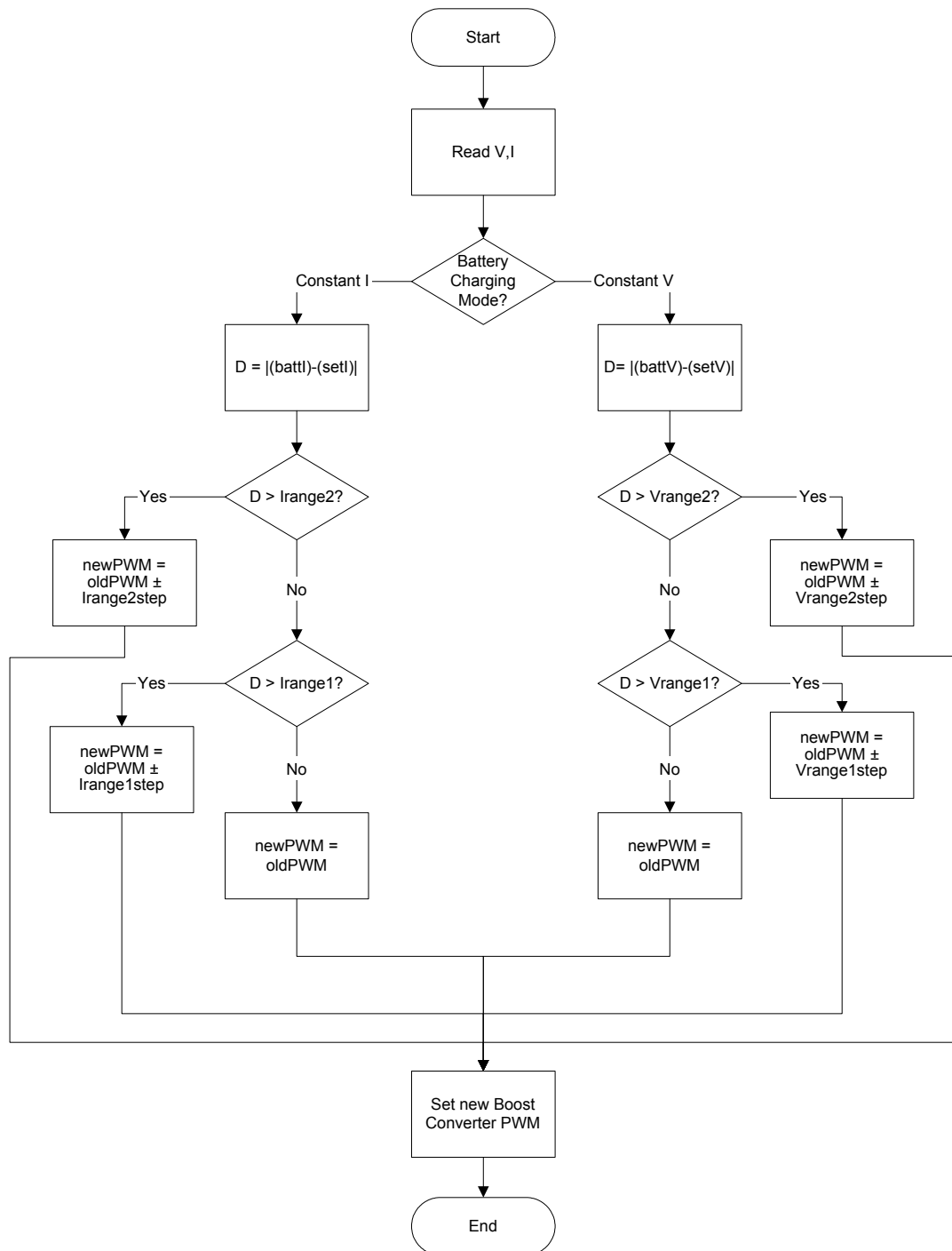


## Appendix D. Data Commands and Packets

Command	Description	Sender	1 <sup>st</sup> Data Byte (Command)	Other Data Bytes
Measurements	Gets battery measurements from a specific battery device.	Base Station	1	-
		Pickup	1	Bytes 2-3: Voltage (mV) Bytes 4-5: Current (mA) Bytes 6-7: Temperature (0.1 °C)
Set Charge	Sets the current/voltage to charge a specific battery with.	Base Station	2	Bytes 2-3: Voltage (mV) Bytes 4-5: Current (mA)
		Pickup	2	-
Battery Type	Gets the type of a specific battery device.	Base Station	3	-
		Pickup	3	Byte 2: Battery Type
Discover – Init	Device Discovery (see Appendix A)	Base Station	6	Byte 2: Number of Slots
Discover – Slot		Base Station	5	Byte 2: Slot Number
		Pickup	5	Byte 2: Slot Number
Discover – Assign		Base Station	4	Byte 2: Slot Number Byte 3: New Comm. ID
		Pickup	4	-
Release ID	Instructs a device to release its Communications ID.	Base Station	7	-
		Pickup	7	-

NB: Multi-byte data is in Big Endian format.

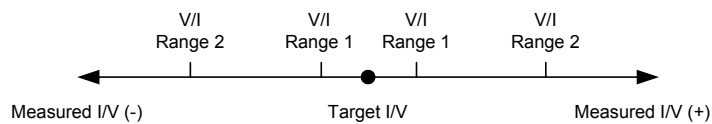
## Appendix E. Current and Voltage Control Algorithm



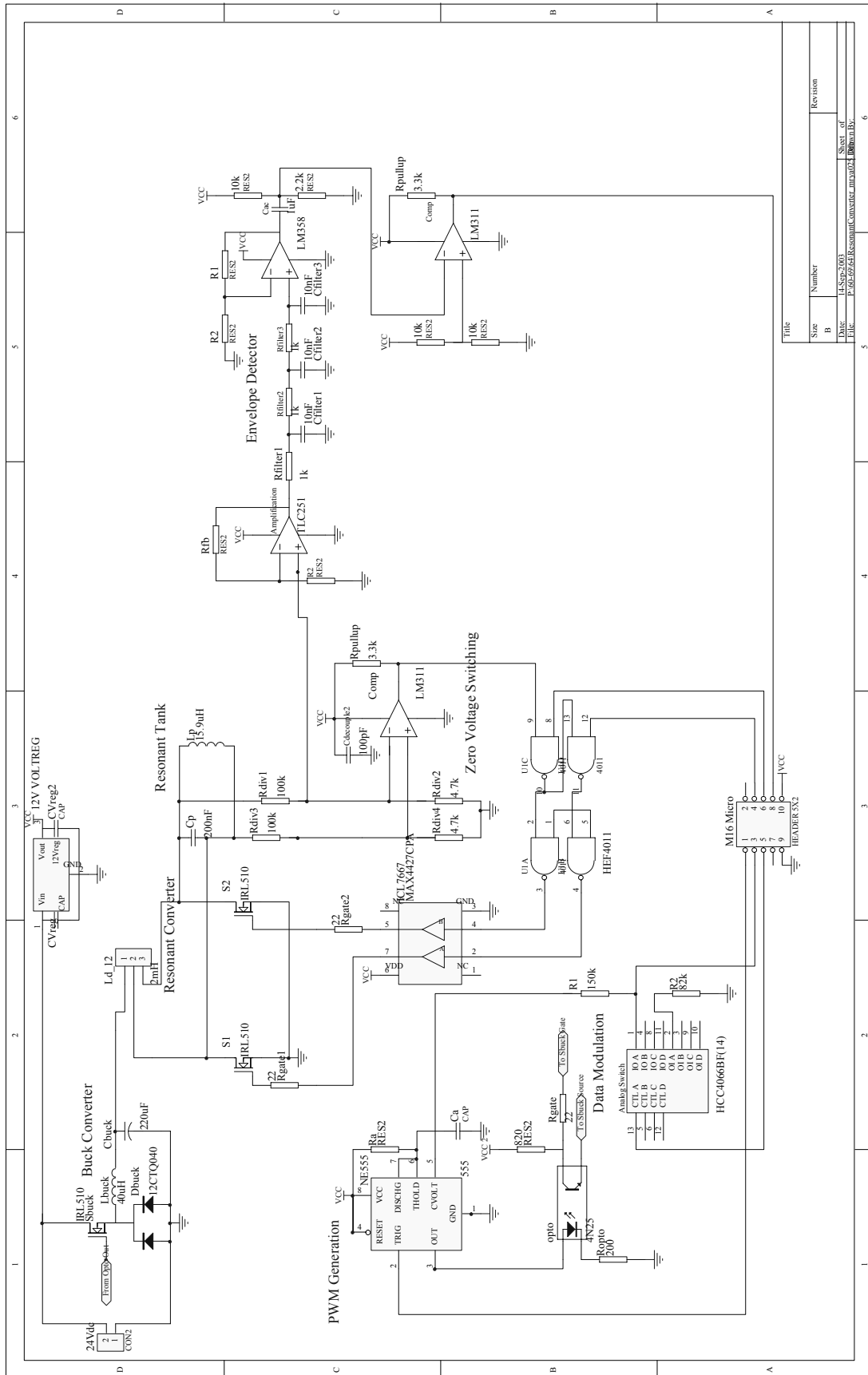
Outside Range 2 - large difference between set I/V and measured I/V, large coefficient of change.

Outside Range 1 - small difference between set I/V and measured I/V, small coefficient of change.

Inside Range 1 - Within PWM change accuracy, no change.



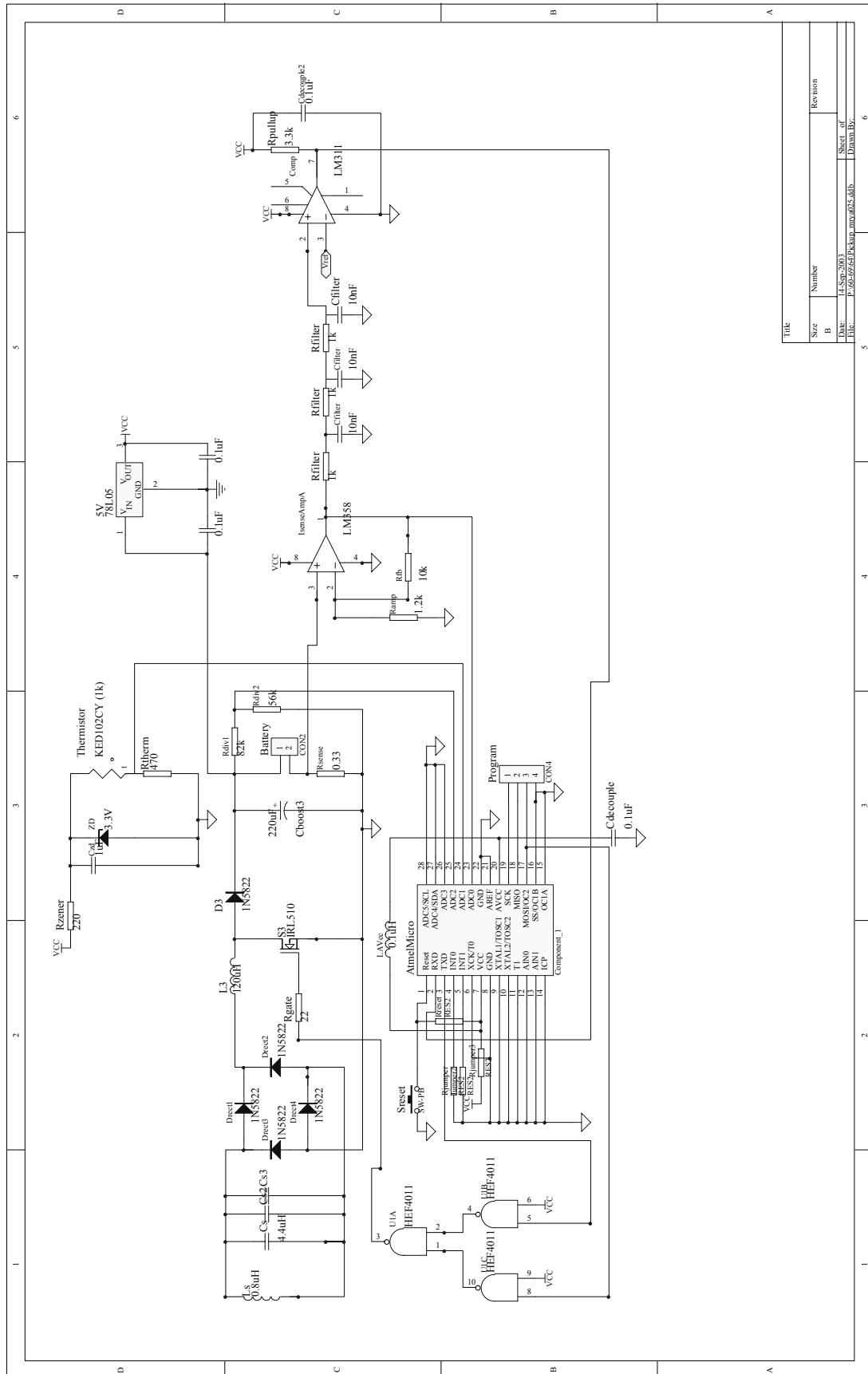
**Appendix F. Base Station Circuit Schematic**



Title	Size	Number	Revision
	B		
Date:	14-Sep-2003	Sheet of	
File:	F:\Project\ResonantConverter\main103.dbrn103	Sheet of	



## Appendix G. Pickup Circuit Schematic



Title		Revision	
Size	Number		
B			
Date:	11-Sep-2003	Sheet of	
DR:	P. BERTZ/EP/Marking/035/001	Drawn by:	